

Review

Open Access



# Challenges and prospects of Mg-air batteries: a review

Yaru Wang<sup>1</sup>, Yukun Sun<sup>1</sup>, Wen Ren<sup>1</sup>, Duo Zhang<sup>1</sup>, Yang Yang<sup>1</sup>, Jun Yang<sup>1</sup>, Jiulin Wang<sup>1</sup>, Xiaoqin Zeng<sup>2,\*</sup>, Yanna NuLi<sup>1,\*</sup> 

<sup>1</sup>School of Chemistry and Chemical Engineering, Shanghai Electrochemical Energy Devices Research Center, Shanghai Jiao Tong University, Shanghai 200240, China.

<sup>2</sup>State Key Laboratory of Metal Matrix Composite, Shanghai Jiao Tong University, Shanghai 200240, China.

\*Correspondence to: Prof./Dr. Yanna NuLi, School of Chemistry and Chemical Engineering, Shanghai Electrochemical Energy Devices Research Center, Shanghai Jiao Tong University, 800 Dongchuan Road, Shanghai 200240, China. E-mail: nlyn@sjtu.edu.cn; Prof./Dr. Xiaoqin Zeng, State Key Laboratory of Metal Matrix Composite, Shanghai Jiao Tong University, 800 Dongchuan Road, Shanghai 200240, China. E-mail: xqzeng@sjtu.edu.cn

**How to cite this article:** Wang Y, Sun Y, Ren W, Zhang D, Yang Y, Yang J, Wang J, Zeng X, NuLi Y. Challenges and prospects of Mg-air batteries: a review. *Energy Mater* 2022;2:200024. <https://dx.doi.org/10.20517/energymater.2022.20>

**Received:** 24 Apr 2022 **First Decision:** 23 May 2022 **Revised:** 6 Jun 2022 **Accepted:** 21 Jun 2022 **Published:** 1 Jul 2022

**Academic Editors:** Yuping Wu, Yun Zhang **Copy Editor:** Tiantian Shi **Production Editor:** Tiantian Shi

## Abstract

Mg-air batteries, with their intrinsic advantages such as high theoretical volumetric energy density, low cost, and environmental friendliness, have attracted tremendous attention for electrical energy storage systems. However, they are still in an early stage of development and suffer from large voltage polarization and poor cycling performance. At present, Mg-air batteries with high rechargeability remain difficult to achieve, mainly because the discharge products [Mg(OH)<sub>2</sub>, MgO and MgO<sub>2</sub>] are thermodynamically and kinetically difficult to decompose at moderate voltage ranges. Therefore, it is crucial to optimize the reaction paths and kinetics from the electrodes to the batteries via the combination of materials design and first-principles calculations. In this review, remarkable progress is highlighted regarding the currently used materials for Mg-air batteries, including anodes, electrolytes, and cathodes. In addition, the corresponding reaction mechanisms are comprehensively surveyed. Finally, future perspectives for rechargeable Mg-air batteries with decreased voltage polarization and improved cycling performance are also described for further practical applications.

**Keywords:** Mg-air batteries, rechargeability, anode, electrolyte, cathode, application



© The Author(s) 2022. **Open Access** This article is licensed under a Creative Commons Attribution 4.0 International License (<https://creativecommons.org/licenses/by/4.0/>), which permits unrestricted use, sharing, adaptation, distribution and reproduction in any medium or format, for any purpose, even commercially, as long as you give appropriate credit to the original author(s) and the source, provide a link to the Creative Commons license, and indicate if changes were made.



## INTRODUCTION

In the context of the vigorous development of electric vehicles and stationary energy storage, the requirements of high theoretical volumetric energy density, low cost, and sustainable electrical energy storage systems have become significant issues<sup>[1-3]</sup>. Among the various electrical energy storage technologies, rechargeable metal-air batteries, whose cathode material is oxygen (O<sub>2</sub>) directly derived from the atmosphere, have attracted significant interest from researchers due to their high theoretical energy densities from the reaction of metal with O<sub>2</sub>. Research into Li-air batteries, which can provide a theoretical specific energy density of 3458 Wh·kg<sup>-1</sup> (based on Li<sub>2</sub>O<sub>2</sub>) and a theoretical working voltage of 2.96 V, has resulted in remarkable achievements in the last few decades<sup>[4]</sup>. However, the development of Li-air batteries faces the challenges of safety issues and the high price of Li anodes. On this basis, the study of other metal-air batteries has also gradually developed, including more secure multivalent metallic anodes, such as zinc, aluminum, and magnesium<sup>[5-9]</sup>. **Table 1** presents a comparison of the electrochemical properties of different metal-air batteries. Among the various rechargeable multivalent metal-air batteries, Mg-air batteries are considered to be “green” power sources of next-generation battery technologies for electric automobiles and large-scale energy storage due to their high theoretical energy densities (14 kWh·L<sup>-1</sup> and 3.9 kWh·kg<sup>-1</sup>, based on MgO)<sup>[8]</sup>. Importantly, Mg has a relatively low redox potential [-2.37 V vs. standard hydrogen electrode (SHE)], low cost (\$0.26 g<sup>-1</sup>)<sup>[10]</sup>, sustainability (2.08% in the Earth’s crust)<sup>[7,8]</sup>, a less reactive nature and resistance to dendrite formation<sup>[11]</sup>.

Primary Mg-air batteries are based on metal magnesium as the anode active material and oxygen in the air as the cathode active material in an aqueous electrolyte, as shown in **Figure 1A**. On the anode side, the Mg metal is oxidized to magnesium ions [Equation 1] and the magnesium ions further combine with hydroxide ions to form magnesium hydroxide [Equation 2] in the aqueous electrolyte:



On the cathode side, the products of aqueous and aprotic electrolytes are different. For aqueous Mg-air batteries, oxygen molecules from the atmosphere, combining electrons and water molecules, are reduced to hydroxide ions, which further unite Mg<sup>2+</sup> from the anode to form Mg(OH)<sub>2</sub> [Equation 3]. In contrast, the discharge products are considered to be MgO and/or MgO<sub>2</sub> in aprotic electrolytes [Equations 4 and 5]<sup>[10,12]</sup>, as shown in **Figure 1B**.



The current issues facing primary Mg-air batteries are reducing the anode corrosion rate mainly caused by the hydrogen evolution reaction (HER) and increasing the discharge voltage. In comparison to the wide studies of Li-air batteries, there have only been a few reports on rechargeable Mg-air batteries<sup>[12-15]</sup>. The reasons for limiting the reversibility of Mg-air batteries are twofold. First, the self-discharge of Mg anodes in aqueous electrolytes results in the formation of insulating Mg(OH)<sub>2</sub> products, which impede further anode reactions. Second, in organic electrolytes, the discharge products MgO ( $\Delta G_f^\ominus = -568.9 \text{ kJ mol}^{-1}$ ) and MgO<sub>2</sub> ( $\Delta G_f^\ominus = -567.8 \text{ kJ mol}^{-1}$ ) are difficult to decompose due to their stable thermodynamics and poor

**Table 1. Comparison of various rechargeable metal-air batteries**

Selected batteries	Theoretical open cell voltage (V vs. SHE)	Theoretical energy density (Wh·kg <sup>-1</sup> )	Reaction
Li-air	2.96	3458	2Li + O <sub>2</sub> ↔ Li <sub>2</sub> O <sub>2</sub>
Mg-air	2.95	3905	2Mg + O <sub>2</sub> ↔ 2MgO
	2.91	2751	Mg + O <sub>2</sub> ↔ MgO <sub>2</sub>
Zn-air	1.65	1090	2Zn + O <sub>2</sub> ↔ 2ZnO
Al-air	2.73	4304	4Al + 3O <sub>2</sub> ↔ 2Al <sub>2</sub> O <sub>3</sub>

The theoretical energy density is based on the total mass of the metal anode and O<sub>2</sub> cathode,  $\epsilon_M = -nFE/\Sigma M$ , where F is the Faraday constant, E is the electrochemical reaction potential, and M is the molecular weight of the reactants. SHE: Standard hydrogen electrode.

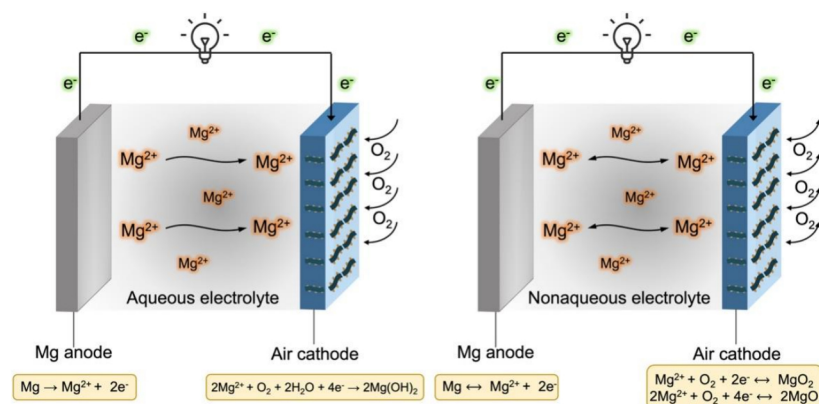


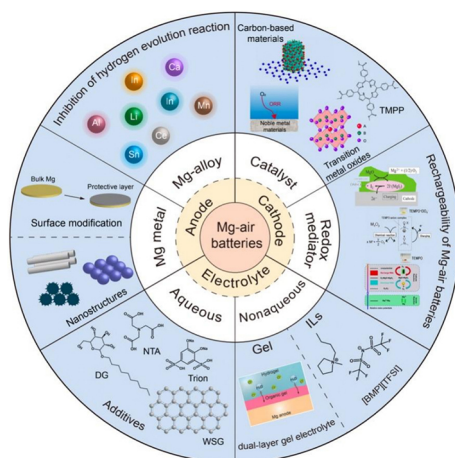
**Figure 1.** Schematic configurations and working principle of (A) aqueous Mg-air batteries and (B) nonaqueous Mg-air batteries.

kinetic properties, resulting in large polarization and poor cycling performance. Current research on rechargeable Mg-air batteries is focused on nonaqueous systems, which are mainly hindered by effective catalysts that are active for the oxygen reduction reaction (ORR) and oxygen evolution reaction (OER) and efficient electrolytes that can provide reversible Mg plating/stripping under an O<sub>2</sub> atmosphere. In recent years, significant progress has been made by the team of Shiga, who first reported rechargeable Mg-air batteries in 2013<sup>[13]</sup>. Other outstanding work by Siegel's group included analyzing of the discharge products and reaction pathways for rechargeable Mg-air batteries through a combination of theoretical calculations and experimental observations<sup>[12,16,17]</sup>.

Several review articles on Mg-air batteries have been published recently from different perspectives<sup>[7,8,18]</sup>. Here, we review the progress made regarding electrode design and electrolyte optimization, as summarized in Scheme 1. There have only been a few reports regarding the separators applied in Mg-air batteries, so they are not discussed here. Furthermore, we discuss the application of Mg-air batteries and further predict the future research directions for rechargeable Mg-air batteries.

## ANODES

The theoretical standard electrode potential of the Mg metal reduction reaction [Equation 1] is -2.37 V vs. SHE. However, owing to the existence of an insulating film [MgO and Mg(OH)<sub>2</sub>] on the surface of the Mg anode originating from the side reaction of metallic Mg with O<sub>2</sub> and H<sub>2</sub>O in the atmosphere, there is always a high level of polarization during the electrochemical Mg plating and stripping process. Therefore, the strategies that can reduce the formation of the passivation layers and improve the properties of Mg itself are crucial to Mg-air batteries.



**Scheme 1.** Schematic of key materials (anode, cathode and electrolyte) for Mg-air batteries. TMPP: tetramethoxyphenyl-porphyrin; WSG: water-soluble graphene; NTA: nitrilotriacetic acid; DG: decyl glucoside; ILs: ionic liquids.

## Mg metal

During the discharge process of the Mg anode in an aqueous electrolyte, a passivation film of  $\text{Mg}(\text{OH})_2$  that inhibits further electrode reactions adheres on the Mg surface. Currently, the materials used for the anode of primary Mg-air batteries are mainly modified Mg metal and Mg alloys, as summarized in Table 2. In order to alleviate the formation of the  $\text{Mg}(\text{OH})_2$  passivation film, researchers have adopted nanostructured Mg with a high specific surface area as an effective anode material. In 2006, Li *et al.* prepared Mg spheres, plates, nanorods, and sea-urchin-like nanostructures [Figure 2A] and tested their electrochemical performance<sup>[19]</sup>. In their work, they prepared various Mg structures with a simple vapor-transport approach and controlled their shape by changing the evaporation temperatures and flow rates of Ar gas. The results indicated that the battery made from Mg sea-urchin-like nanostructures exhibited a higher energy density ( $565 \text{ Wh}\cdot\text{kg}^{-1}$ ) and a better high-rate discharge capability compared with the battery made from Mg powder, which was attributed to the porous network structure.

A 100 nm porous Mg thin film was reported for an alkaline primary Mg-air battery by Xin *et al.* in 2013<sup>[20]</sup>. The morphologies of the Mg films were controlled by adjusting the deposition temperatures [Figure 2B] and the performance of Mg-air batteries based on Mg film anodes was tested. The Mg films deposited at  $150^\circ\text{C}$  exhibited a high open-circuit voltage (OCV) of 1.41 V and a large discharge capacity of  $821 \text{ mAh}\cdot\text{g}^{-1}$ , as illustrated in Figure 2C. It is noteworthy that the porous network of these nanostructures not only reduces the anodic polarization of Mg electrode but also increases the activity of Mg itself, thus increasing the utilization efficiency of the Mg electrode. Nonetheless, these works only alleviate the formation of the passivation film but cannot fundamentally solve the passivation problem of Mg anodes in aqueous electrolytes. Although the passivation film is also observed in conventional organic electrolytes, reversible Mg plating and stripping can be accomplished in specific organic electrolytes (i.e., ethers as the solvents) that are suitable for rechargeable Mg-air batteries.

Another strategy to improve the performance of the Mg anode is to modify its surface, which is in contact with the electrolyte. In a study by Zhao *et al.* in 2021, a bismuth (Bi)-based artificial protective layer, which is electrically insulative but ionically conductive, on the Mg metal anode was explored in a magnesium bis(trifluoromethanesulfonyl)imide ( $\text{Mg}(\text{TFSI})_2$ )/diglyme (G2) organic electrolyte<sup>[21]</sup>. It was found that the modified Mg anode had better cycling stability than the pristine Mg anode due to the inhibition of the harmful parasitic reaction between the Mg metal and  $\text{Mg}(\text{TFSI})_2$ -based electrolyte. Furthermore, the

**Table 2. Important recent studies of various anodes for primary Mg-air batteries**

	Materials	Morphology	Synthesizing method	Discharge performance	Year
Mg metal	Mg nanoparticles <sup>[19]</sup>	Spheres, plates, nanorods and sea-urchin-like <sup>[19]</sup>	Vapor-transport approach	Sea-urchin-like Mg nanoparticles achieved a high open-circuit voltage of 1.42 V and a high energy density of 565 Wh·kg <sup>-1</sup> at a current density of 5 mA·cm <sup>-2</sup>	2006
	Mg thin film <sup>[20]</sup>	Porous Mg thin film with a thickness of 100 nm	Using magnetron sputtering (at different substrate temperatures)	Mg thin film prepared at 150 °C achieved a high open-circuit voltage of 1.41 V and a large specific discharge capacity of 821 mAh·g <sup>-1</sup> at 0.1 mA·cm <sup>-2</sup>	2013
Mg-alloy	Mg-Ca <sup>[23]</sup>	Cylinder	Melting at 750 °C under protection gas	Mg-0.1Ca achieved a high open-circuit voltage of 2.032 V, a stable cell voltage of 1.6 V at 0.5 mA·cm <sup>-2</sup> and a specific energy density of 1429 Wh·kg <sup>-1</sup> at a current density of 10 mA·cm <sup>-2</sup>	2018
	Mg-14Li-Al-0.1Ce <sup>[33]</sup>	Sheet (with a thickness of 1.5 mm)	Commercial purchase	Mg-Li-Al-Ce anode achieved an operating voltage of 1.272 V, a specific discharge capacity of 2076 mAh g <sup>-1</sup> and an anodic utilization efficiency of 85.2% at 2.5 mA·cm <sup>-2</sup>	2011
	Mg-Al-Pb-In <sup>[34]</sup>	Sheet	Melting at 730 °C under protection gas	Mg-Al-Pb-In anode achieved an open-circuit voltage of 1.88 V and a peak power density of 94.5 mW·cm <sup>-2</sup>	2014
	Mg-Al-Sn-Mn <sup>[36]</sup>	Cylinder	Melting at 740 °C under protection gas and refining agent hexachloroethane	The optimal combination Mg-6Al-1Sn-0.4Mn achieved a discharge potential of -1.602 V	2018

tolerance to water was improved, which was of positive significance for the application of Mg-air batteries in real environments with non-pure oxygen [Figure 2D-F]. This modified Mg anode shows significant potential for rechargeable Mg-air batteries.

### Mg alloys

In addition to the concerted efforts focused on the particles, morphologies, and surface film of Mg, alloying Mg with elements with a high hydrogen evolution overpotential is attracting growing attention. The Mg-alloy prepared by doping pure magnesium with metals or elements (i.e., Al, Zn, Ga, Ca, Pb, Li, Mn, and rare earth elements) can effectively inhibit the HER and self-corrosion reactions of the anode, thereby facilitating the self-peeling of the discharge products and thus reducing the polarization of Mg anodes in aqueous electrolytes<sup>[22-31]</sup>. There have been many studies on Mg-Zn<sup>[22]</sup>, Mg-Ca<sup>[23]</sup>, commercial AZ31 (Mg-3%Al-1%Zn), AZ61 (Mg-6%Al-1%Zn)<sup>[24,25]</sup>, and AP65 (Mg-6%Al-5%Pb)<sup>[26]</sup> alloys serving as anodes for Mg-air batteries and significant effort has also been devoted to some other elements with high corrosion resistance<sup>[27-34]</sup>. For example, a Mg-Li alloy (13 wt.% Li) exhibited a more negative standard electrode potential *vs.* SHE and higher anodic efficiency. A battery with this Mg-Li alloy offered a higher operating voltage and capacity than those with the conventional Mg-Al alloy<sup>[31]</sup>. The addition of Mn helped to reduce the corrosion rate via the incorporation of low-soluble metals in the Al-Mn intermetallic phases<sup>[32]</sup>.

Furthermore, Ma and colleagues<sup>[33]</sup> successfully fabricated a Mg-14Li-Al-0.1Ce alloy and found that a Mg-air battery with this alloy exhibited an operating voltage (1.261 V) and specific discharge capacity (2076 mAh·g<sup>-1</sup>) than those of Mg and AZ31. As shown in Figure 3A, the corrosion potential of Mg-Li-Al-Ce (-1.625 V) was more negative than that of Mg (-1.572 V) and AZ31 (-1.505 V), with Mg-Li-Al-Ce exhibiting the smallest anodic Tafel slope of all samples, thereby revealing its higher electrochemical activity. Furthermore, the discharge products loosely adhered to the alloy electrode surface, so the electrolyte was able to penetrate through to contact the electrode. Wang *et al.* found that a Mg-Al-Pb-In alloy with a finer grain structure showed a more negative discharge potential and stronger discharge activity compared with a Mg-Al-Pb alloy<sup>[34]</sup>. Indium played an important role in diminishing the self-discharge rate of the Mg-Al-Pb alloy and thus improved its utilization efficiency. In addition, weak polarizability was observed for the Mg-

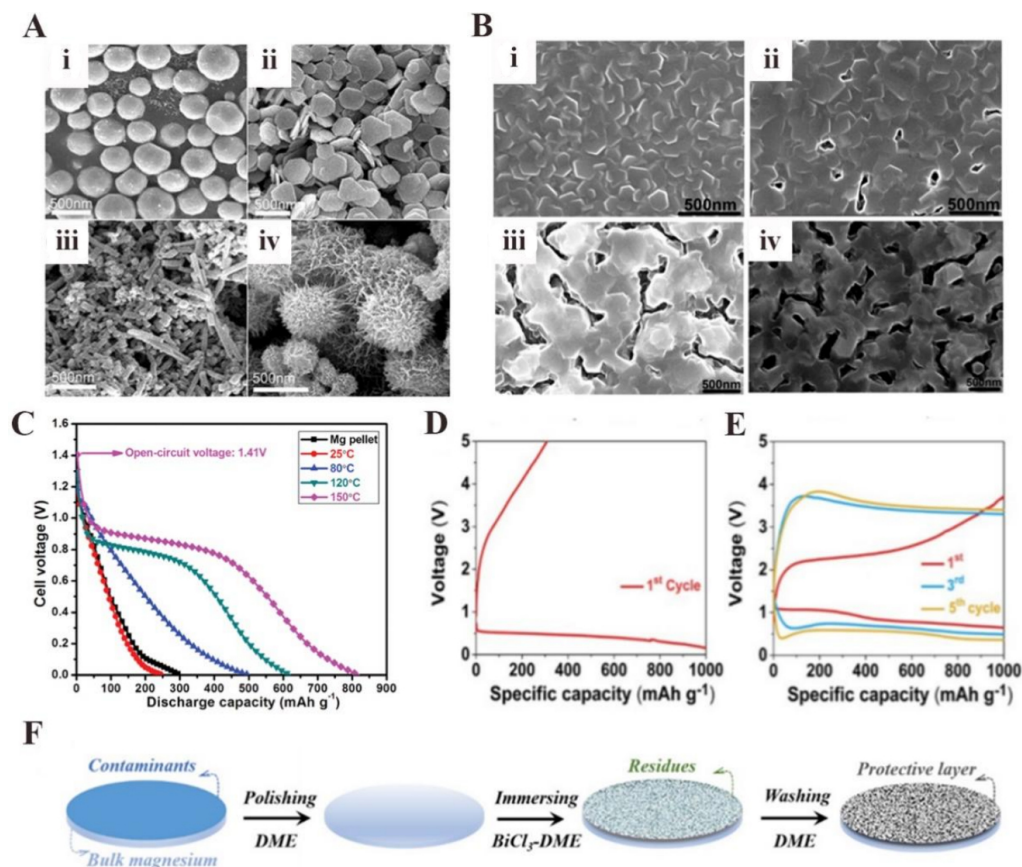


**Figure 2.** (A) Scanning electron microscopy (SEM) images of as-prepared nano Mg anode with different morphologies: (i) sphere-like; (ii) plate-like; (iii) rod-like; (iv) sea urchin-like<sup>[19]</sup>. (B) SEM images of Mg thin films prepared at different substrate temperatures: (i) 25 °C; (ii) 80 °C; (iii) 120 °C; (iv) 150 °C<sup>[20]</sup>. (C) Discharge profiles of primary Mg-air batteries with Mg thin films prepared at different substrate temperatures, showing that the Mg thin films prepared at 150 °C performed the best<sup>[20]</sup>. Charge/discharge profiles of rechargeable Mg-air batteries at 200 mA·g<sup>-1</sup> using (D) pristine Mg with a Mg(TFSI)<sub>2</sub>/G2 electrolyte under pure O<sub>2</sub> and (E) Bi-based protective modified Mg with a Mg(TFSI)<sub>2</sub>/G2 electrolyte under pure O<sub>2</sub><sup>[21]</sup>. (F) Schematic diagram of the preparation of a Bi-based protective layer on a Mg anode<sup>[21]</sup>. Reproduced from Refs.<sup>[19-21]</sup> with permission from Wiley, the Royal Society of Chemistry, and the American Chemical Society, respectively. DME: Dimethoxyethane.

Al-Pb-In alloy with the smallest anodic Tafel slope, which contributed to active behavior during Mg dissolution [Figure 3B]. A Mg-air battery with the Mg-Al-Pb-In alloy anode possessed a high power density of 94.5 mW·cm<sup>-2</sup> in aqueous electrolytes.

In addition to the composition of Mg alloys, their microstructure also has an impact on their electrochemical properties<sup>[35,36]</sup>. For a Mg-Al-Sn anode, the fine Mg<sub>2</sub>Sn phases and fully recrystallized microstructure accelerated the self-peeling of corrosion products, leading to high discharge voltages at high current densities<sup>[37]</sup>. In a study of the precipitate distribution in AZ91 (Mg-9%Al-1%Zn) investigated by Yuasa *et al.*, it was observed that the formation of densely distributed β-precipitates during the discharge process suppressed the corrosion rate<sup>[38]</sup>. In general, fine grains and uniform grain boundaries were valuable for producing high activated currents of the magnesium alloy in aqueous electrolytes<sup>[36,37]</sup>. Due to the good corrosion resistance, Mg-alloy anodes are widely used in aqueous Mg-air batteries. However, there have been few reports of Mg alloys in organic electrolytes for rechargeable Mg-air batteries due to the different restraining factors in the two systems.

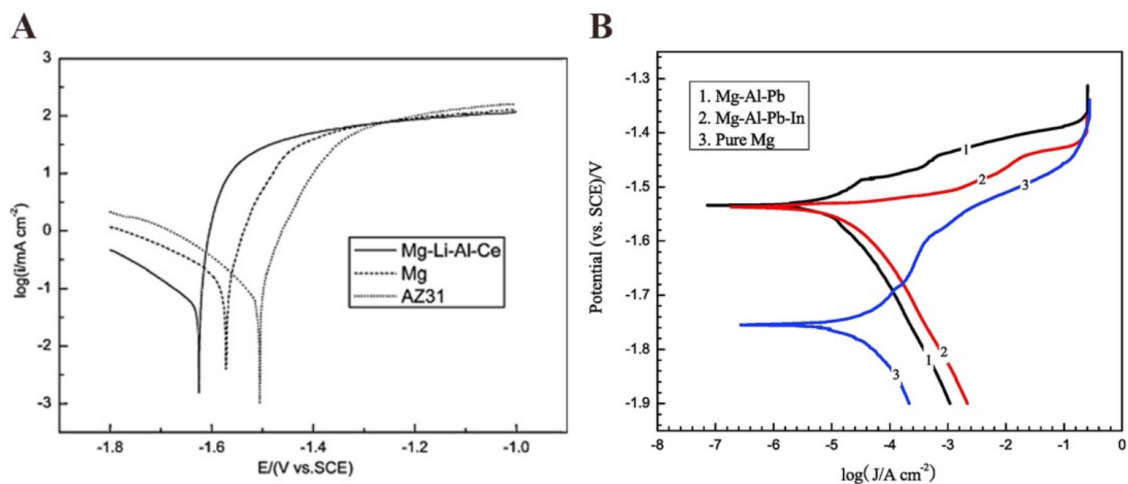


**Figure 3.** Potentiodynamic polarization curves for (A) Mg, AZ31, and Mg-Li-Al-Ce<sup>[33]</sup>. (B) Mg-Al-Pb, Mg-Al-Pb-In alloys and pure magnesium<sup>[34]</sup> measured in a 3.5 wt.% NaCl solution at a scan rate of 1 mV·s<sup>-1</sup>. Reproduced from Refs.<sup>[33,34]</sup> with permission from Elsevier.

## ELECTROLYTES

The electrolyte plays a prominent role in battery electrochemistry, so a suitable electrolyte is essential for a battery system. In this section, according to the water content, the electrolytes for Mg-air batteries are classified into aqueous and nonaqueous electrolytes.

### Aqueous electrolytes

In aqueous electrolytes, the Mg anode undergoes a self-corrosion process, which leads to the formation of magnesium hydroxide on the surface of magnesium and hinders further anodic reactions. Aqueous Mg-air batteries are only regarded as primary batteries since the potential necessary for decomposing magnesium hydroxide results in massive corrosion and H<sub>2</sub> evolution on Mg. Current research on aqueous electrolytes is focused on reducing the anode corrosion and lowering the anodizing overpotentials at the current densities required for practical applications. Here, we summarize the mechanism of Mg corrosion and the corresponding electrolytes.

#### *Causes of anode corrosion and corresponding electrolytes*

For aqueous Mg-air batteries, the Mg electrode is extremely susceptible to corrosion, and thus a high level of polarization is displayed. Through the study of the corrosion behavior of magnesium metal in aqueous solutions<sup>[39-43]</sup>, it can be seen that the causes of magnesium anode corrosion are the HER, negative difference effect (NDE), and the presence of impurities.

The HER process can be described as:



This reaction causes the self-discharge of the Mg electrode and thus decreases the Faradaic efficiency in anodic discharge. Moreover, as the potential of the anode increases during the discharge process of the battery, the rate of H<sub>2</sub> evolution increases, and correspondingly, the corrosion rate of magnesium increases. This phenomenon is known as the NDE. Furthermore, the impurities in the Mg plate are also a factor in accelerating Mg corrosion. Microcells are constructed when impurity phases contact Mg, resulting in low

Mg utilization. Reducing the corrosion of magnesium is essential to improving the Faradaic efficiency of the batteries. On this basis, researchers have made significant efforts to determine the effect of anions in electrolytes on Mg corrosion and search for corrosion inhibitors.

The anions in the solutions affect the corrosion and anodic polarization of Mg anodes. The Mg passivation in aqueous electrolytes with NaCl, NaNO<sub>3</sub>, Na<sub>2</sub>HPO<sub>4</sub>, and a NaCl/Na<sub>3</sub>PO<sub>4</sub> mixture was compared via differential electrochemical mass spectrometry and H<sub>2</sub> pressure rise measurements. It was indicated that the Mg anode in the NaCl solution exhibited the highest H<sub>2</sub> evolution rate as a result of Cl<sup>-</sup> attacking the Mg surface. In contrast, Na<sub>2</sub>HPO<sub>4</sub> and NaNO<sub>3</sub> electrolytes reduced the H<sub>2</sub> evolution corrosion reaction, as illustrated in [Figure 4A](#). [Table 3](#)<sup>[44,45]</sup> summarizes the OCV of pure Mg in various aqueous electrolytes. The pure Na<sub>2</sub>HPO<sub>4</sub> electrolyte increased the Mg<sup>2+</sup> Faradaic efficiency compared to the NaCl electrolyte but introduced extraordinarily large overpotentials during discharge, probably by introducing a resistive layer. The NaNO<sub>3</sub> electrolyte could inhibit Mg corrosion while simultaneously allowing Mg<sup>2+</sup> dissolution during battery discharge. However, a low OCV was exhibited resulting from a NO<sub>3</sub><sup>-</sup> to NO<sub>2</sub><sup>-</sup> reaction<sup>[44]</sup>. MgCl<sub>2</sub>, MgBr<sub>2</sub>, KHCO<sub>3</sub>, NH<sub>4</sub>NO<sub>3</sub>, NaNO<sub>2</sub>, Na<sub>2</sub>SO<sub>4</sub>, and Mg(NO<sub>3</sub>)<sub>2</sub>-NaNO<sub>2</sub> solutions were also studied in previous research<sup>[46]</sup>. NO<sub>3</sub><sup>-</sup>, NO<sub>2</sub><sup>-</sup>, and HPO<sub>4</sub><sup>2-</sup> had higher Faradaic efficiency than Cl<sup>-</sup> and ClO<sub>4</sub><sup>-</sup>. The cell based on a Mg(NO<sub>3</sub>)<sub>2</sub>-NaNO<sub>2</sub> electrolyte exhibited a 90% Faradaic efficiency for the Mg anode with no serious passivation behavior at a discharge current density of 20 mA·cm<sup>-2</sup>, so the Mg(NO<sub>3</sub>)<sub>2</sub>-NaNO<sub>2</sub>-based electrolyte was considered as a good choice for primary Mg-air batteries.

Several reports have revealed the use of organic compounds as effective corrosion inhibitors in aqueous electrolytes<sup>[47-49]</sup>. Deyab reported that the addition of decyl glucoside (DG) to a 3.5 wt.% NaCl electrolyte could reduce the Mg corrosion rate with 94% inhibition efficiency<sup>[47]</sup>. As an organic surfactant, the presence of DG could increase the activation energy of the corrosion reaction. The DG surfactant adsorbed on the Mg surface and the alkyl groups in the DG structure could shield the surface from attack, thereby improving the inhibition efficiency. The Mg-air batteries containing the DG surfactant offered higher operating voltages, discharge capacities, and anodic utilization than in its absence [[Figure 4B](#)]. Analogously, the addition of disodium 4,5-dihydroxy-1,3-benzenedisulfonate (Tiron) and nitrilotriacetic acid (NTA) into an aqueous Mg-air battery electrolyte improved the battery discharge potentials [[Figure 4C](#)] due to the formation of strong complexes with Mg<sup>2+</sup>. In addition to this, the enhancement could be attributed to the suppression of the enrichment and redeposition of Fe on the Mg anode and deactivating Fe-rich impurities that act as cathodic micro-sites, consequently suppressing the NDE phenomenon of the Mg anode<sup>[48]</sup>. Furthermore, the efficiency of Mg-air batteries can be improved by adding water-soluble graphene (WSG) to the NaCl electrolyte as an inhibitor [[Figure 4D](#)]<sup>[49]</sup>. The WSG enhanced the electrical conductivity of the NaCl electrolyte, prevented the magnesium breakdown during the self-discharge, and decreased the corrosion rate of the Mg anode. With an in-depth understanding of the corrosion mechanism, it is expected that research into effective additives will not only decrease the corrosion rate but also improve battery performance.

Aqueous electrolytes are of particular interest because of their high operation safety, excellent ionic conductivity, low cost, and environmental friendliness<sup>[50]</sup>. Furthermore, in the case that rechargeability is still difficult to achieve, the study of aqueous electrolytes has significant application value for primary Mg-air batteries. For primary Mg-air batteries, mainly using aqueous electrolytes, researchers have focused on promoting the utilization of Mg, reducing the corrosion rate, and elevating the operating voltage. Since the key is to inhibit the HER process, there are two promising approaches that can achieve great effects. One is to modify the Mg anodes through methods, including surface modification, doping other metal elements, and changing electrode morphologies. The other approach is to study the effect of electrolytes and design

**Table 3. OCVs of pure Mg in various aqueous electrolytes**

Electrolyte	OCV of Mg (V vs. Ag/AgCl)	Ref.
0.5 M NaCl	-1.61	[44]
0.5 M NaCl/0.05 M Na <sub>2</sub> HPO <sub>4</sub>	-1.58	[44]
0.5 M Na <sub>2</sub> HPO <sub>4</sub>	-1.52	[44]
0.5 M NaNO <sub>3</sub>	-1.40	[44]
0.1 M Na <sub>2</sub> SO <sub>4</sub>	-1.50	[45]

OCV: Open-circuit voltage.

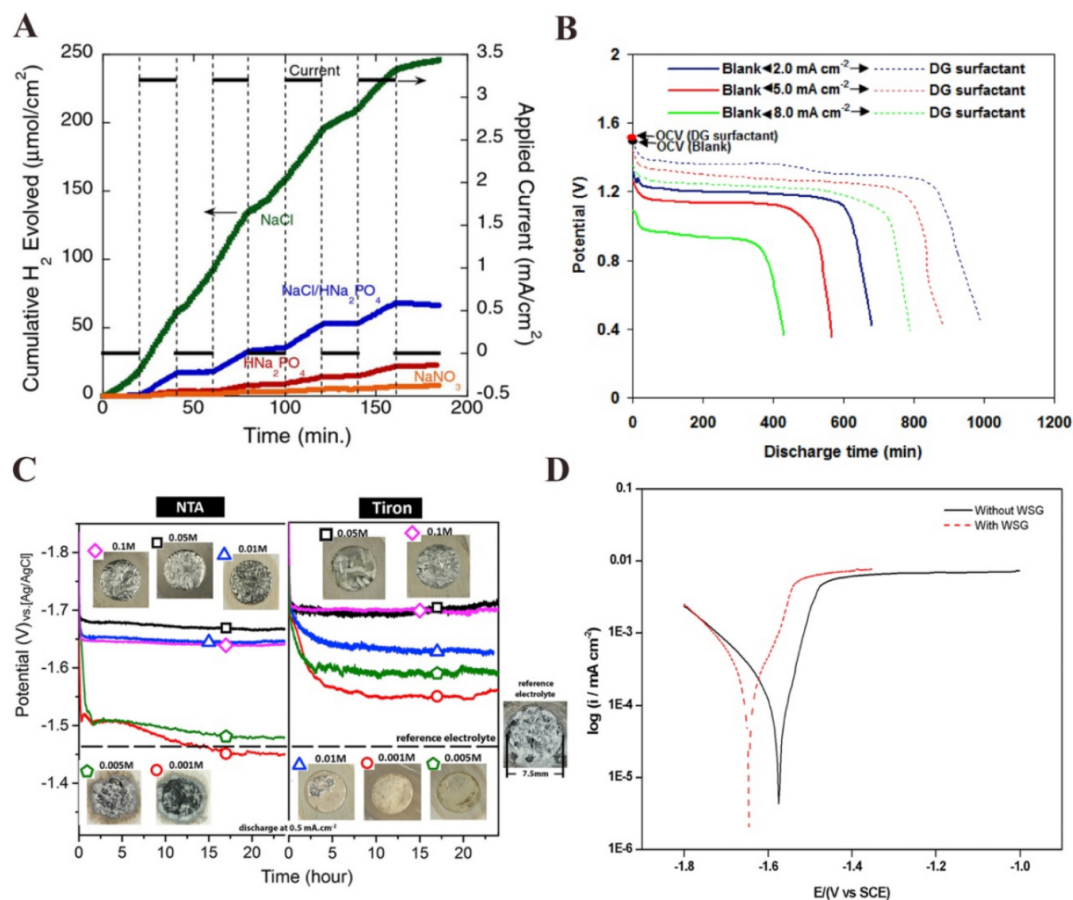


**Figure 4.** (A) H<sub>2</sub> evolution from a Mg working electrode in 0.5 M NaCl (green), 0.5 M NaCl + 0.05 M Na<sub>2</sub>HPO<sub>4</sub> (blue), 0.5 M Na<sub>2</sub>HPO<sub>4</sub> (red) and 0.5 M NaNO<sub>3</sub> (orange) electrolytes<sup>[44]</sup>. (B) Discharge profiles of Mg-air batteries working with electrolytes with/without DG additives under different current densities<sup>[47]</sup>. (C) Discharge profiles of commercial pure Mg with NTA and Tiron electrolyte additives at concentrations of 0.001, 0.005, 0.01, 0.05, and 0.1 M. The insets show macrographs of the anode surface after 24 h<sup>[48]</sup>. (D) Potentiodynamic polarization profiles for Mg anode in a 3.5% NaCl electrolyte with and without WSG<sup>[49]</sup>. Reproduced from Refs<sup>[47,49]</sup> with permission from Elsevier. NTA: Nitriiotriacetic acid.

electrolytes with proper anions or additives that can inhibit corrosion without retarding Mg<sup>2+</sup> dissolution in aqueous electrolytes.

### Nonaqueous electrolytes

The self-corrosion of Mg anodes severely inhibits the reversibility of Mg-air batteries in aqueous electrolytes, and therefore, nonaqueous electrolytes have been introduced to the design of rechargeable Mg-

air batteries. Different from aqueous electrolytes, molecular H<sub>2</sub>O is not included in the reaction paths and the discharge products are mainly composed of magnesium oxides or peroxides, as shown in Equations 4 and 5. For the design of rechargeable Mg-air batteries, a suitable electrolyte needs to achieve three requirements. First, the electrolyte should be compatible with the Mg anode, which ensures the reversibility of Mg<sup>2+</sup> plating/stripping from the Mg anode. Second, since Mg-air batteries work under an open system, the electrolyte must be sustainable enough to endure the whole ORR/OER process under the O<sub>2</sub> atmosphere. Third, a low viscosity and volatility, wide electrochemical window, and high ionic conductivity should be obtained. In addition to the traditional solution-phase electrolyte systems, gel-polymer and ionic liquid electrolytes have shown excellent prospects in rechargeable Mg-air batteries.

#### *Organic electrolytes*

Although the electrolytes of rechargeable magnesium batteries (RMBs) are greatly recommended for applications in nonaqueous Mg-air batteries, the main problem is the passivation of the Mg anode in organic electrolytes. The reversibility of RMBs greatly depends on the solid-electrolyte interface (SEI) formed during the first discharge process. Unfortunately, the SEI layer formed by the reaction between Mg and most electrolytes cannot support the fast diffusion of Mg<sup>2+</sup>, becoming the passivation layer, which in turn severely inhibits the reversibility of the Mg plating/stripping process. Lu *et al.* researched the impact of organic solvents and salts in electrolytes on the Mg anode, and they found that the electrochemical properties of RMBs were mainly restricted by the passivation layer on the Mg anode and both the solvents (i.e., esters, sulfones, and amides) and the salts (i.e., BF<sub>4</sub><sup>-</sup>, PF<sub>6</sub><sup>-</sup>, and AsF<sub>6</sub><sup>-</sup>) would passivate the Mg anode<sup>[51]</sup>. Thus, the necessity of designing electrolytes compatible with Mg anodes is self-evident.

Current rechargeable Mg-air batteries are realized in nonaqueous electrolytes<sup>[12-15]</sup>. In the first research into rechargeable Mg-air batteries, dimethyl sulfoxide (DMSO) was used as the solvent that could form complexes with iodine molecules<sup>[13]</sup>. The complex could catalyze the decomposition of the discharge products, as further discussed in Section "Redox mediators: one solution to achieve reversibility of Mg-air batteries". Mg(ClO<sub>4</sub>)<sub>2</sub>, as the supporting salt for Mg plating/stripping, shows relatively lower overpotentials than TFSI<sup>[15]</sup>, so it has been applied in Mg-air batteries. Furthermore, the temperature conditions of Mg-air batteries should also be taken into consideration. 0.5 M magnesium bis(trifluoromethanesulfonyl)amide [Mg(TFSA)<sub>2</sub>] in diethyl-methyl-methoxymethylpiperidium trifluoromethane sulfonylamide was applied in rechargeable Mg-air batteries reported by Shiga *et al.* due to their stable Mg plating/stripping at 60 °C<sup>[14]</sup>. Vardar *et al.* applied a (PhMgCl)<sub>4</sub>-Al(OPh)<sub>3</sub>/tetrahydrofuran (THF) electrolyte in their Mg-O<sub>2</sub> batteries because of its high Coulombic efficiency of Mg plating/stripping<sup>[12]</sup>. In 2016, Vardar *et al.* employed a MgCl<sub>2</sub>/AlCl<sub>3</sub>/dimethoxyethane electrolyte for Mg-O<sub>2</sub> cells and showed that the discharge capacity of this system was greatly improved compared to cells with modified Grignard electrolytes<sup>[52]</sup>. However, the reversibility was severely limited, which could be attributed to the oxygen diffusion in the electrolyte forming an insulation film that was difficult to decompose on the surface of the anode.

In summary, the composition of the electrolytes greatly affects the performance of Mg-air batteries. It is necessary to ensure Mg plating/stripping with low overpotentials under O<sub>2</sub> atmospheres whilst ensuring that the catalysts are compatible with the organic electrolytes.

#### *Gel-polymer electrolytes*

Metal-air batteries with gel-polymer electrolytes offer the advantages of safety, high energy density, and flexible design. In view of the mature research and application of polymer electrolytes for Li-air batteries<sup>[53]</sup>, gel-polymer electrolytes have also drawn great interest from researchers for Mg-air batteries<sup>[54,55]</sup>.

Liew *et al.* designed an economical, inherently safe, and environmentally benign biopolymer WSG-incorporated agar gel electrolyte for Mg-air batteries<sup>[54]</sup>. They investigated the effect of agar concentrations on electrolyte performance. The Mg corrosion resistance was increased in the WSG-incorporated agar gel electrolytes [Figure 5A] due to the stable electrode/electrolyte interface. The Mg-air battery with the optimal gel electrolyte (WSG-incorporated 3% w/v agar) exhibited a high OCV in the range of 1.6-1.7 V and a discharge capacity of 1010.60 mAh·g<sup>-1</sup> [Figure 5B]. In 2021, Li *et al.* reported a Mg-air battery with the highest average specific capacity (2190 mAh·g<sup>-1</sup>) and energy density (2282 Wh·kg<sup>-1</sup>) so far, as shown in Figure 5C and D<sup>[55]</sup>. The outstanding performance was achieved by designing a dual-layer gel electrolyte that consisted of a poly(ethylene oxide) organic gel and a crosslinked polyacrylamide hydrogel [Figure 5E]. The organic gel could reduce the corrosion rate and the chlorine ions in the hydrogel helped to produce unique needle-like discharge products that ensured the active Mg could closely contact the electrolyte during the discharge process, resulting in the improved discharge capacity.

### *Ionic liquid electrolytes*

Ionic liquids (ILs) are ionic compounds that are liquid at room temperature and therefore have high conductivity to both inorganics and organics<sup>[56-58]</sup>. Compared with traditional organic electrolytes, ILs have a wider liquid path, lower vapor pressure and flammability, higher thermal stability, and wider electrochemical window, and thus have been applied in various battery systems (i.e., lithium-ion batteries<sup>[59,60]</sup>, sodium-ion batteries<sup>[61]</sup>, magnesium-ion batteries<sup>[62,63]</sup>, metal-air batteries<sup>[64-66]</sup> and metal-sulfur batteries<sup>[67,68]</sup>).

For primary Mg-air battery research, IL-based electrolytes have been investigated to be available for making Mg interfacial films more stable<sup>[69,70]</sup>. Furthermore, introducing oligomeric ether additives or using ether-functionalized ionic liquid cations can promote reversible Mg deposition and dissolution. In these electrolytes, ether oxygen can replace the TFSI<sup>-</sup> anion in the Mg<sup>2+</sup> coordination domain<sup>[71]</sup>. Kar *et al.* designed a safe, non-volatile electrolyte based on Mg[BH<sub>4</sub>] interacting with an ether functionalized IL, specifically [N<sub>2</sub>(<sub>20201</sub>)(<sub>20201</sub>)(<sub>20201</sub>)] [NTf<sub>2</sub>]<sup>[72]</sup>. It was demonstrated that stable magnesium cycling in this IL displayed over 20 cycles, producing a Coulombic efficiency of 60%. Recent research indicated that Mg<sup>2+</sup>/IL electrolytes with high ionic conductivity could facilitate Mg stripping and plating at a low overpotential<sup>[73,74]</sup>.

In 2016, Law *et al.* explored the ORR and OER in butyl-1-methylpyrrolidinium bis(trifluoromethanesulfonyl)imide ([BMP][TFSI])-based electrolytes with and without Mg<sup>2+</sup> ions on polycrystalline Au and glassy carbon electrodes in a three-electrode configuration and discussed their implications on the cathodic processes in Mg-air batteries<sup>[75]</sup>. In the absence of Mg<sup>2+</sup>, the ORR currents were stable and the reversible one-electron transfer process could be attributed to the reduction of O<sub>2</sub> into the superoxide anion O<sub>2</sub><sup>-</sup> (O<sub>2</sub> + e<sup>-</sup> ↔ O<sub>2</sub><sup>-</sup>). While in the Mg<sup>2+</sup> (Mg(TFSI)<sub>2</sub>)-containing [BMP][TFSI] electrolyte, the ORR was irreversible due to the formation of passivation layers limiting the diffusion of O<sub>2</sub> and O<sub>2</sub><sup>-</sup> to/away from the electrode surfaces. The morphology and the chemical composition of the deposits formed on the electrodes after the voltammetric measurements were characterized. It was suggested that no MgO or MgO<sub>2</sub> was observed as an ORR product except MgF<sub>2</sub> as the main deposit, which indicated the decomposition of TFSI<sup>-</sup> ions was more favorable. The result was revealed via chemical analysis of the electrode surfaces after the ORR<sup>[75]</sup>.

In 2018, the same group further investigated the activity of different electrode materials (Pt, Au, GC, Mn<sub>2</sub>O<sub>3</sub>, and MnO<sub>2</sub>) in a rotating ring disk electrode setup. In the pure [BMP][TFSI] electrolyte, a reversible ORR and OER were observed in all electrodes, while in the electrolyte containing Mg<sup>2+</sup> [Mg(TFSI)<sub>2</sub>], the OER of all electrode materials was strongly hindered. They found that the OER did not occur due to the irreversible reactions of the electrolyte with the ORR products, resulting in the passivation film formation and

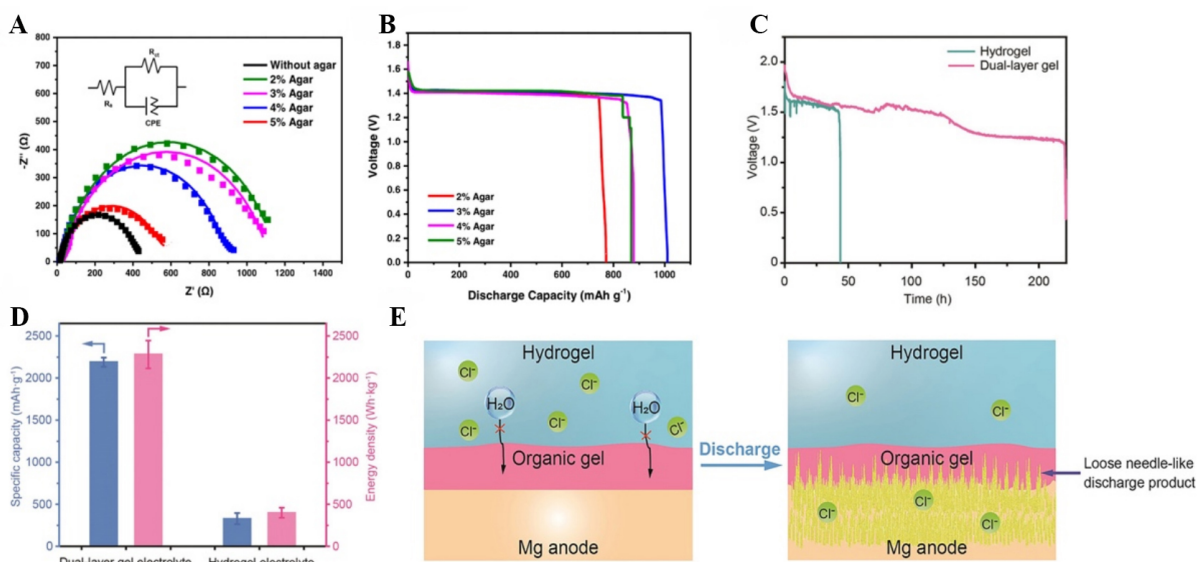


**Figure 5.** (A) Electrochemical impedance spectroscopy spectra of Mg strips immersed in different WSG-incorporated agar gel electrolytes<sup>[54]</sup>. (B) Discharge performance of Mg-air batteries with different WSG-incorporated agar gel electrolytes at the current density of 11.11 mA·cm<sup>-2</sup><sup>[54]</sup>. (C) Discharge curves of Mg-air batteries applying dual-layer gel and hydrogel electrolytes<sup>[55]</sup>. (D) Specific capacity and energy density of Mg-air batteries using dual-layer gel and hydrogel electrolytes<sup>[55]</sup>. (E) Schematic diagram of the mechanism of how the dual-layer gel electrolyte protects the Mg anode from corrosion, indicating the needle-like discharge products formed on the anode during discharge, which provide fresh active Mg<sup>[55]</sup>. Reproduced from Refs.<sup>[54,55]</sup> with permission from Springer Nature and Wiley, respectively.

inactivation of the electrode surface. The morphology and chemical composition of the electrode surfaces were characterized after cycling the potential from 1.2 to 0.6 V vs. Mg/MgO for five cycles in O<sub>2</sub>-saturated 0.1 M Mg(TFSI)<sub>2</sub>/[BMP][TFSI] electrolyte via SEM and X-ray photoelectron spectroscopy (XPS). It was indicated that MgO<sub>2</sub> was the main product of the ORR process<sup>[76]</sup>. It is noteworthy that the results of XPS evidenced a negligible amount of MgF<sub>2</sub> for all electrodes studied, which contradicted their previous findings<sup>[75]</sup>.

In 2019, Jusys *et al.* further researched the ORR on an Au film electrode in [BMP][TFSI] via a differential electrochemical mass spectrometry and *in situ* infrared spectroscopic model study<sup>[77]</sup>. In O<sub>2</sub>-saturated [BMP][TFSI], the reduction of O<sub>2</sub> to peroxide anions occurred at a more negative potential. The adsorption characteristics of IL ions and the exchange dynamics were greatly affected by the anions formed during the ORR process. In the additional presence of Mg<sup>2+</sup> ions, the ORR became irreversible, resulting from the formation of MgO<sub>2</sub> and MgO. MgO<sub>2</sub> was confirmed to be the main ORR product, which was consistent with their previous research<sup>[76]</sup>. In addition, the formation of MgF<sub>2</sub> was also revealed via *in situ* infrared (IR) spectroscopy.

These studies suggest that the main reason for the irreversibility of the ORR in Mg<sup>2+</sup>-containing [BMP][TFSI] is that the ORR products cannot be decomposed, thereby hindering the diffusion of O<sub>2</sub> and O<sub>2</sub><sup>-</sup>. Therefore, the future directions for rechargeable Mg-air batteries are research into Mg<sup>2+</sup>-containing ILs that favor the decomposition of ORR products and the exploration of effective bifunctional catalysts, which are discussed in subsequent sections.

## AIR CATHODES

Compared to the Mg anode and electrolyte, the air cathode is the key component restricting the development of metal-air batteries so far. It has been demonstrated that the energy storage capacity and power capability of Mg-air batteries are strongly dependent on the properties of air electrodes, which are affected by their architecture and catalytic materials.

### Typical structure of an air cathode

A typical air cathode includes four layers, namely, a waterproof layer, a gas diffusion layer, a catalyst layer, and a current collector layer<sup>[7]</sup>, as shown in [Figure 6](#). The waterproof layer is used to separate the electrolyte and air as well as to be permeable only to O<sub>2</sub> and block CO<sub>2</sub> and H<sub>2</sub>O. The gas diffusion layer has a high porosity and a high electronic conductivity to ensure the fast diffusion of oxygen from outside to the catalyst surface.

### Catalysts

The catalyst layer in the air cathode is a pivotal component that influences the electrocatalysis of the ORR on the air cathode of Mg-air batteries. The ORR is a complex process that includes many electrochemical and chemical steps, and different intermediates are produced during the process. The slow kinetics of ORR, which is related to the catalyst type, surface state, and structure of the air cathode, is the main reason for the low Faradaic efficiency and Coulombic efficiency of Mg-air batteries. Possible pathways for ORR include a two-electron pathway [Equation 4] and a four-electron pathway [Equations 3 and 5]<sup>[78,79]</sup>. Whether the electrochemical reaction of air cathode is carried out via a four-electron pathway or a two-electron pathway depends mainly on the type and state of the catalysts<sup>[79]</sup>.

#### *Types of catalysts for primary Mg-air batteries*

The most common air cathode catalysts for primary Mg-air batteries are noble metal materials, transition metal oxides, nitrogen-containing metal macrocycles, and carbon-based materials.

Pt-based materials are effective catalysts with high activity towards the ORR and have been widely researched in fuel cells and metal-air batteries<sup>[80-82]</sup>. Pt functioning as a catalyst directly will certainly increase the cost of Mg-air batteries; therefore, Pt-based alloys and nanostructures are used to reduce the Pt content and improve the catalytic performance simultaneously. To date, many groups have studied the ORR activity of Pt alloys, such as Pt-Co<sup>[83]</sup>, Pt-Ni<sup>[84]</sup>, Pt-Cu<sup>[85]</sup>, Pt-Y<sup>[86]</sup>, and so on. Furthermore, the Mo element was introduced to Pt/C to enhance the catalytic activity [[Figure 7A](#)] of Pt/C by increasing the density of Pt-5d band vacancies and segregating Pt on the particle surface of the Pt-Mo alloy<sup>[87]</sup>. When the Pt-Mo/C catalyst was applied to Mg-air batteries, the discharge voltage plateau obviously improved compared to Pt/C, as shown in [Figure 7B](#).

The high price of Pt limits the wide-scale commercialization potential of Mg-air batteries. Therefore, low-cost non-Pt noble metal materials with a high ORR activity have been widely researched for practical applications. Ag and Cu exhibit weak ORR catalyst activity individually, but they become active toward the ORR in alkaline conditions when alloyed at the nanoscale. Qaseem *et al.*<sup>[88]</sup> reviewed the progress of silver nanoalloy electrocatalysts for the ORR in alkaline media, focusing on the mechanism of the ORR and the factors that impair the ORR activity. Pd, which is much cheaper, has been reported in a number of studies and considered as a substitute for Pt these years<sup>[89]</sup>. When Pd particles are highly dispersed, the catalytic activity of Pd is similar to Pt supported on graphite at the same weight<sup>[90]</sup>. Furthermore, it has been reported that Pd/C is available for higher catalytic activity than Pt/C either in acidic media<sup>[91]</sup> or alkaline solutions<sup>[92]</sup>.

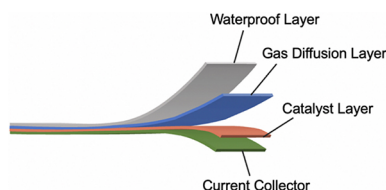


**Figure 6.** Schematic diagram of the structure of a typical air cathode including a waterproof layer, a gas diffusion layer, a current collector layer, and a catalyst layer<sup>[7]</sup>.

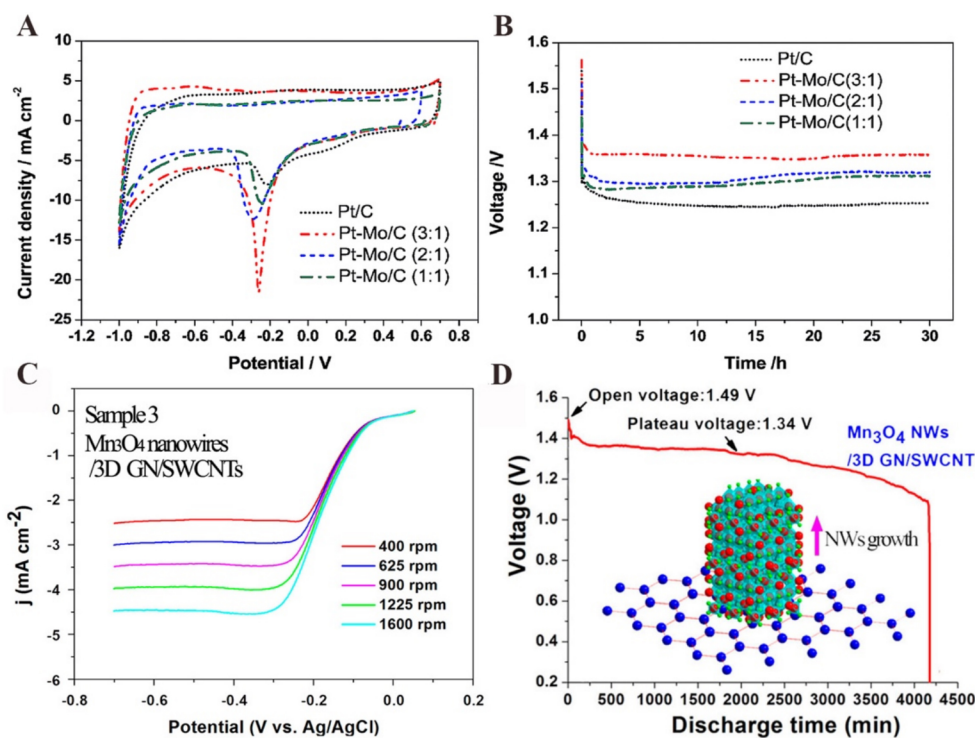


**Figure 7.** (A) Cyclic voltammograms of electrodes with different Pt-Mo-based catalysts in an  $O_2$ -saturated 3.5 wt.% NaCl aqueous solution at a scanning rate of  $50 \text{ mV}\cdot\text{s}^{-1}$ <sup>[87]</sup>. (B) Discharge profiles of Mg-air batteries using different Pt-Mo-based catalysts at a current density of  $5 \text{ mA}\cdot\text{cm}^{-2}$  in a 3.5 wt.% NaCl electrolyte<sup>[87]</sup>. (C) Rotating-disk voltammograms of  $Mn_3O_4$  NW/3D GN/SWCNTs in  $O_2$ -saturated 0.1 M KOH at a sweep rate of  $10 \text{ mV}\cdot\text{s}^{-1}$  and different rotation rates<sup>[94]</sup>. (D) Discharge profile of Mg-air batteries using  $Mn_3O_4$  nanowires/three-dimensional graphene/single-walled carbon nanotube ( $Mn_3O_4$  NW/3D GN/SWCNT) catalysts in a mixed electrolyte of  $Mg(NO_3)_2$  (2.6 M) and  $NaNO_2$  (3.6 M) with the additive of 1.0 wt.% [P6,6,6,14][Cl] ionic liquid. The inset illustration is the schematic diagram of the controllable growth of one-dimensional  $Mn_3O_4$  nanowires on graphene in the microwave field<sup>[94]</sup>. Reproduced from Refs<sup>[87,94]</sup> with permission from RSC Publishing and the American Chemical Society, respectively.

Transition metal oxides are relatively inexpensive and stable, as well as an important type of non-precious metal ORR catalysts, of which manganese oxides are the most commonly used. The oxygen reduction catalytic performance of different structures of  $MnO_2$  is in the order of  $\beta$ - <  $\lambda$ - <  $\gamma$ - <  $\alpha$ - $MnO_2$ , according to Cao *et al.*<sup>[93]</sup>. The oxygen reduction performance of  $MnO_2$  is related to the structures and morphologies. Nanoscale particles have more oxygen reduction active sites owing to the higher specific surface area and porosity than microscale particles<sup>[94]</sup>. The doping of low-cost metal elements (such as Ni<sup>[95]</sup>, Cu<sup>[96]</sup>, and so on) in manganese oxides can enhance their catalytic activity. However, a key disadvantage of manganese oxides as cathode catalysts is their low conductivity. To solve this problem, the commonly used method is to combine manganese oxide and a carrier with good conductivity, such as porous carbon and graphene<sup>[97]</sup>. Li *et al.* reported  $Mn_3O_4$  nanowires/three-dimensional graphene/single-walled carbon nanotube ( $Mn_3O_4$

NWs/3D GN/SWCNT) electrocatalysts<sup>[94]</sup>. The calculated kinetic current density observed for Mn<sub>3</sub>O<sub>4</sub> NWs/3D GN/SWCNT reached 51.8% of the Pt/C value. The electron transfer number was close to ~4.0, suggesting a four-electron pathway for the ORR. Mg-air batteries based on Mn<sub>3</sub>O<sub>4</sub> NWs/3D GN/SWCNT cathode catalyst displayed a high cell open-circuit voltage (1.49 V) and a high plateau voltage (1.34 V), as shown in [Figure 7C](#) and [D](#).

Nitrogen-containing metal macrocycles are considered a potential substitute for Pt for ORR catalysts. The Fe- and Co-based macrocycles, such as tetramethoxyphenyl-porphyrin (TMPP<sup>[98]</sup>), tetraphenylporphyrin (TPP<sup>[99]</sup>), and phthalocyanine (Pc<sup>[100]</sup>), have been of great research significance. High-temperature treated metal macrocycles have good oxygen reduction activity and stability, and the coordination of nitrogen and transition metal ions provides catalytic active sites. A high-surface-area CoTMPP/C catalyst fabricated by ultrasonic spray pyrolysis possessed higher oxygen reduction activities than Pt/C<sup>[101]</sup>. Boukoureshtlieva *et al.* applied CoTMPP as the cathode catalyst for Mg-air batteries and found that the Mg-air battery based on cobalt (II) tetramethoxyphenyl porphyrin pyrolyzed on an active carbon (AC/CoTMPP) cathode catalyst could generate currents of 2.5-140 A and power of up to 154 W<sup>[98]</sup>.

Carbon materials are ubiquitous in the air cathodes of Mg-air batteries and can work not only as conductive agents and gas diffusion layers but also as catalysts directly. As catalysts, two-electron electroreduction tends to occur on the surface of carbon<sup>[102]</sup>. However, the efficiency of the two-electron pathway is relatively low because the formation of HO<sub>2</sub><sup>-</sup> during the two-electron pathway can oxidize the active substance in the air electrode. Therefore, the carbon material itself is not a good oxygen reduction catalyst. Despite this, due to high specific surface area and excellent conductivity, carbon materials are excellent catalyst carriers that can produce synergistic catalytic effects with noble metals<sup>[90-92]</sup> and transition metal compounds<sup>[94,97]</sup> deposited on the surface. Furthermore, nitrogen-doped carbon materials also have relatively high ORR activity, probably because the dissociation energy of O<sub>2</sub> molecular can be reduced by the nitrogen atoms<sup>[103,104]</sup>.

#### *Redox mediators: one solution to achieve reversibility of Mg-air batteries*

In organic solvents, Mg<sup>2+</sup> interacts with oxygen molecules through a four-electron pathway [Equation 5] or a two-electron pathway [Equation 4] and the products (MgO, MgO<sub>2</sub>) adhere to the air cathode surface. MgO and MgO<sub>2</sub> are both difficult to decompose at ambient temperatures due to their thermodynamical and electrochemical stability<sup>[17]</sup>. In order to solve this issue, redox mediators (RMs) were used to reduce the reaction barrier for the decomposition of the discharge products<sup>[13-15]</sup>.

The first rechargeable Mg-air batteries were reported by Shiga *et al.* in 2013<sup>[13]</sup>. Using the iodine-DMSO complex as a charging catalyst, they charged a nonaqueous Mg-air battery in a 0.5 mol·L<sup>-1</sup> Mg(ClO<sub>4</sub>)<sub>2</sub>/DMSO electrolyte at 60 °C. The charging mechanism could be described by:



The charge process was realized by the catalytic property of I<sub>2</sub>-DMSO complex, which reacts with MgO to form MgI<sub>2</sub> and thus promotes the evolution of O<sub>2</sub>, as shown in [Figure 8A](#). It was suggested that MgO could be removed from the cathode at ~2.0 V and the cell could sustain four galvanostatic cycles [[Figure 8B](#)]. In 2014, Shiga *et al.* further proposed a rechargeable Mg-O<sub>2</sub> battery with 2,2,6,6-tetramethylpiperidine-1-oxyl (TEMPO) working as a mediator at 60 °C<sup>[14]</sup>. They firstly demonstrated that MgO could be decomposed under the catalysis of TEMPO-anion complex (PTMA<sup>+</sup>ClO<sub>4</sub><sup>-</sup>) [[Figure 8C](#)], which was detected by gas chromatography-mass spectrometry (GC/MS) and inductively coupled plasma atomic emission spectroscopy (ICP-AES). When applied the TEMPO-anion complex as a charge mediator to the Mg-O<sub>2</sub>

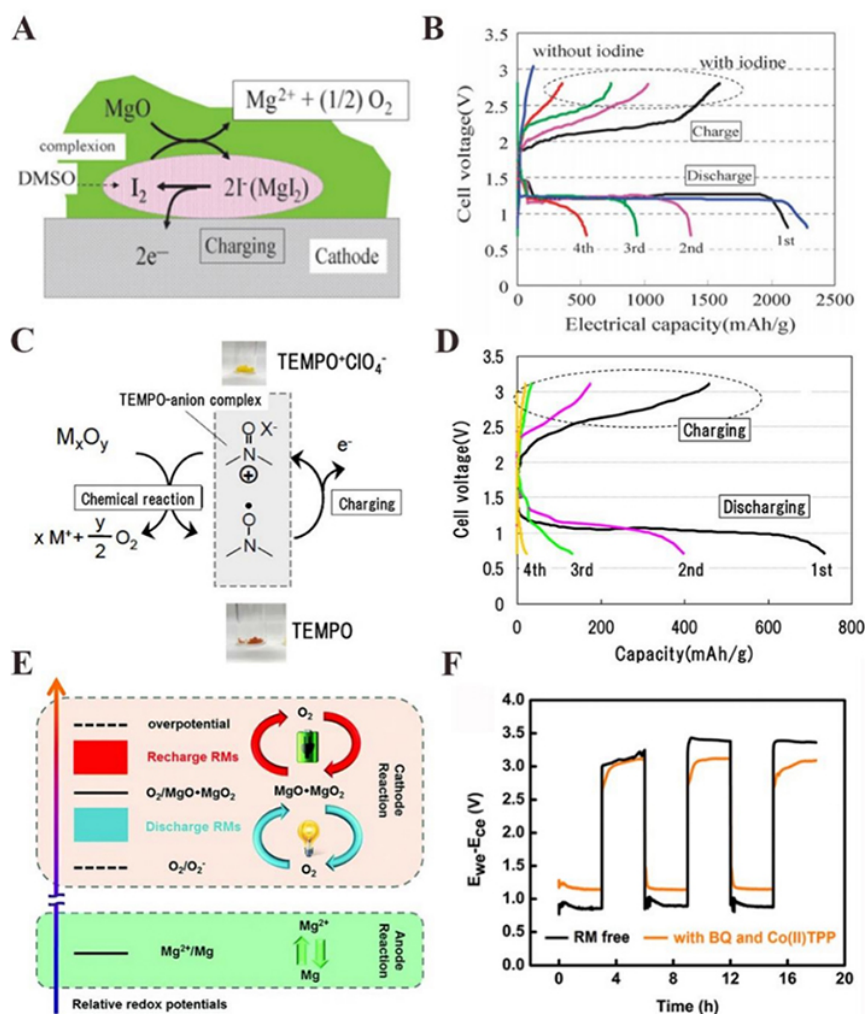


**Figure 8.** (A) Schematic diagram of  $I_2$ -DMSO complex catalytic mechanism<sup>[13]</sup>. (B) Discharge-charge profiles of Mg-air batteries with/without iodine at  $60^\circ C$ <sup>[13]</sup>. (C) Schematic diagram of TEMPO-anion complex catalytic mechanism<sup>[14]</sup>. (D) Discharge-charge profiles of the Mg-air battery incorporating PTMA in the cathode at  $60^\circ C$ <sup>[14]</sup>. (E) Schematic diagram of BQ and Co(II)TPP dual redox mediator working mechanism<sup>[15]</sup>. (F) Galvanostatic cycling of the Mg-air battery using BQ and Co(II)TPP dual redox mediators. The voltage profile of the working electrode (carbon paper) was measured against the counter electrode (Mg ribbon) in a two-electrode configuration<sup>[15]</sup>. Reproduced from Refs.<sup>[13-15]</sup> with permission from the Royal Society of Chemistry, the American Chemical Society, and the Royal Society of Chemistry, respectively. TEMPO: 2,2,6,6-tetramethylpiperidine-1-oxyl.

battery, the battery incorporating poly(2,2,6,6-tetramethylpiperidinyloxy methacrylate) (PTMA) in the cathode with  $0.5 \text{ mol}\cdot\text{L}^{-1} \text{ Mg}(\text{TFSI})_2$  in diethyl-methyl-methoxymethylpiperidium bis(trifluoromethanesulfonyl)imide electrolyte at  $60^\circ C$  could be run for four cycles and the discharge capacity of the first cycle was  $737 \text{ mAh}\cdot\text{g}^{-1}$  [Figure 8D]. They suggested that the capacity loss was due to the incomplete decomposition of discharge products.

To facilitate the discharge and recharge processes of Mg-air batteries, Dong *et al.* used 1,4-benzoquinone (BQ) and 5,10,15,20-tetraphenyl-21H,23H-porphine cobalt(II) (Co(II)TPP) dual redox mediators to reduce the overpotential of the discharge process and the charge process, respectively [Figure 8E]<sup>[15]</sup>. This battery exhibited at least three cycles, and the overpotentials for discharge and recharge both achieved a 0.3 V reduction [Figure 8F].

Reducing the reaction barrier by introducing RMs to Mg-air batteries opens a door for rechargeable Mg-air batteries. However, rechargeable Mg-air batteries still face the challenges of low discharge voltage and poor cycle performance, which can be ascribed to the formation of superoxides, the passivation on Mg anodes, and the sluggish kinetics of ORR/OER, so it is worthwhile devoting more effort to this.

#### *Candidates for rechargeable Mg-air batteries: bifunctional catalysts*

The bifunctional catalysts for both the ORR and OER are under intensive investigation in various systems as essential components for rechargeable metal-air batteries. However, there are few reports on the application of bifunctional catalysts for Mg-air batteries. Considering the similarity between Mg-air batteries and other metal-air batteries, such as Li- and Zn-air batteries, here, we discuss some bifunctional catalysts that shed light on further research on rechargeable Mg-air batteries.

Among various metal bifunctional catalysts, noble metals still present excellent catalytic effects for both the ORR and OER. Zhao *et al.* used the couple of 40 wt.% Pt/C and 40 wt.% RuO<sub>2</sub> as cathode catalysts in their research for the Mg anode with a bismuth-based protective layer and the fabricated Mg-O<sub>2</sub> batteries exhibited significant charge-discharge reversibility<sup>[21]</sup>. Du *et al.* compared the catalytic activity of catalysts with different proportions of Pt and IrO<sub>2</sub>, and eventually found that the addition of IrO<sub>2</sub> depressed the ORR catalytic ability while enlarged the stability of OER. Besides, among all the tested catalysts, the pure Pt nanoparticles showed the greatest ORR catalytic effect<sup>[105]</sup>. Noble metal alloys have also attracted the attention of researchers. Kang *et al.* used density functional theory (DFT) calculations to study the effect of Pt<sub>3</sub>M (M = 3d, 4d, and 5d transition metals) catalysts on the kinetics of the ORR and OER for Li-air batteries<sup>[106]</sup>. It turned out that the fifth subgroup elements were the most efficient alloy components, and the outstanding catalytic effect derived from the electron-rich catalyst surface, proposing the direction for the design of bifunctional catalysts for Mg-air batteries. Non-noble metal bifunctional catalysts have attracted much attention these years due to their lower cost than noble metals. Li *et al.* used a hydrothermal-incineration method to synthesize Co/Fe nanoparticles compounded in an N-doped carbon framework (Co/Fe@NC)<sup>[107]</sup>. The N-doped carbon-based material not only improved the electric conductivity but also provided numerous mesoporous channels for discharge products. Thus, the rechargeable Li-air batteries based on Co/Fe@NC catalyst achieved excellent electrochemical performance with a low overpotential (~1.003 V), long cycle life (250 cycles), and high capacity (17326 mAh·g<sup>-1</sup>) [Figure 9A]. Chen *et al.* synthesized a bifunctional electrocatalyst of graphite nanoarrays-confined Fe and Co single atoms within graphene sponges (FeCo-NGS) through a self-assembly technique<sup>[108]</sup>. The FeCo-NGS catalyst enabled the rechargeable Zn-air batteries with a long cycle of more than 1500 hours at a 10 mA·cm<sup>-2</sup> current density, a non-noticeable voltage fading and a low voltage gap of 0.89 V.

Transition metal compounds are always considered promising candidates for bifunctional catalysts. Among them, Mg-, Co- and Ni-based catalysts are studied extensively. Xu *et al.* adjusted the parameters of the first-step hydrothermal reaction to synthesize the hortensia-like MnO<sub>2</sub> interwove with carbon nanotubes [Figure 9B]<sup>[109]</sup>. The MnO<sub>2</sub>/CNT catalyst showed primary electrochemical properties when applied to the rechargeable Zn-air batteries [Figure 9C], which could be attributed to the higher electronic conductivity supported by CNTs and the more active sites provided by the unique morphology of the catalyst. It also pointed out that the morphology of MnO<sub>2</sub> greatly impacted the catalytic effect, which is consistent with the findings reported by Débart *et al.*<sup>[110]</sup>. Zhu *et al.* deposited the nanosized MnO<sub>2</sub> particles on reduced graphene oxide (rGO), taking advantage of the porous layered structure of rGO, and applied them to the rechargeable Li-air batteries<sup>[111]</sup>. The battery catalyzed by MnO<sub>2</sub>@rGO presented an initial discharge capacity of 5139 mAh·g<sup>-1</sup> and retained about 80% of the capacity (4262 mAh·g<sup>-1</sup>) after 15 full discharge-charge cycles at a current density of 100 mA·g<sup>-1</sup>. Kim *et al.* developed an N-doped open structure cobalt and nickel

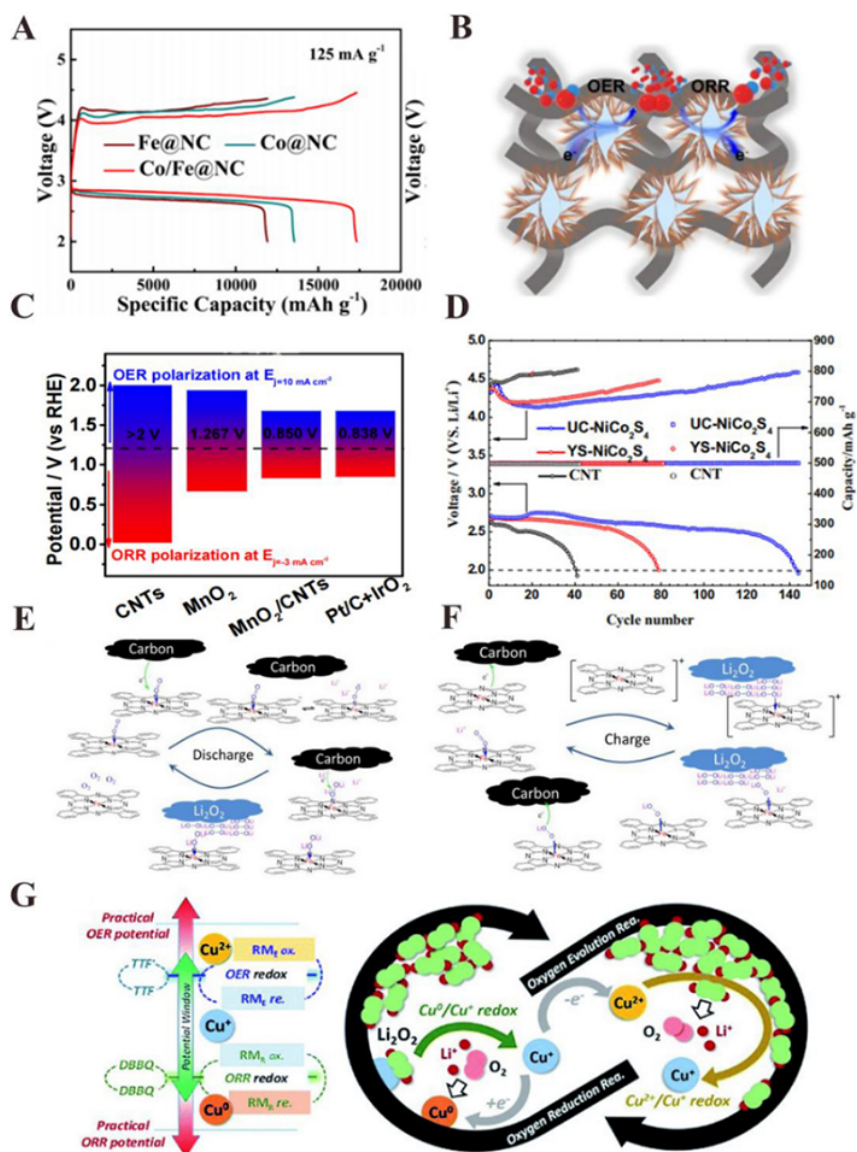


**Figure 9.** (A) Charge/discharge profiles of rechargeable Li-air batteries working with Fe@NC, Co@NC, and Co/Fe@NC catalysts in a 1 M LiTFSI/G4 electrolyte at a current density of 125 mA g<sup>-1</sup>. (B) Schematic diagram of ORR and OER processes catalyzed by MnO<sub>2</sub>/CNTs. (C) Comparison of OER and ORR bifunctional activities (ΔE) of different catalysts including pure CNTs, pure MnO<sub>2</sub>, hortensia-like MnO<sub>2</sub>/CNT, and noble metal catalysts. (D) Cycling performances of Li-air batteries working with UC-NiCo<sub>2</sub>S<sub>4</sub>, YS-NiCo<sub>2</sub>S<sub>4</sub>, and CNT in 1 M LiTFSI/G4 electrolyte at a current density of 100 mA g<sup>-1</sup> and a controlled capacity of 500 mAh g<sup>-1</sup>. Schematic diagrams of the possible catalyzed reaction routes of Li-air batteries working with iron phthalocyanine (FePc) in the electrolyte, discharge process (E), and charge process (F). (G) Schematic diagram of the proposed redox mediation mechanisms for copper ions in Li-air batteries. Reproduced from Refs. [107,109,114,116,117] with permission from the American Chemical Society, IOP Science, American Chemical Society, and the Royal Society of Chemistry, respectively. ORR: Oxygen reduction reaction; OER: oxygen evolution reaction.

bimetallic nanocage (CNBN), which showed better electrochemical catalytic performance than pure cobalt oxide, nickel oxide, and the noble metal Pt/C<sup>[112]</sup>. Furthermore, the CNBN catalyst might present a promising future when applied to rechargeable metal-air batteries, as it was mentioned.

Perovskite oxides have also been widely studied in the field of metal-air batteries. Fan *et al.* reported the  $\text{Sm}_{0.5}\text{Sr}_{0.5}\text{Co}_{1-x}\text{Fe}_x\text{O}_{3-\delta}$ /acetylene black catalyst<sup>[113]</sup>. Thanks to the good synergistic effect of perovskite oxide  $\text{Sm}_{0.5}\text{Sr}_{0.5}\text{Co}_{1-x}\text{Fe}_x\text{O}_{3-\delta}$  and acetylene black, the catalyst showed good catalytic activity for the ORR and OER and maintained the catalytic effect after long cycling (more than 1000 cycles).

Transition metal sulfides also show excellent catalytic activity for the ORR and OER. Sulfur atoms have lower electronegativity and a larger radius than oxygen atoms, and therefore, sulfides seem to have higher electronic conductivity and cell volume than oxides. However, studies on sulfide catalysts mainly focus on rechargeable Li-air batteries at present. Xu *et al.* prepared urchin-like  $\text{NiCo}_2\text{S}_4$  (UC- $\text{NiCo}_2\text{S}_4$ ) and yolk-shell  $\text{NiCo}_2\text{S}_4$  nanospheres (YS- $\text{NiCo}_2\text{S}_4$ ), and both showed excellent catalytic activity for the ORR and OER<sup>[114]</sup>. With the help of spinel sulfide catalysts, the rechargeable Li-air batteries realized more than 140 cycles (limited capacity of  $500 \text{ mAh}\cdot\text{g}^{-1}$ ) with a low voltage gap (lower than 1.5 V) at a current density of  $100 \text{ mA}\cdot\text{g}^{-1}$ , as shown in Figure 9D. The UC- $\text{NiCo}_2\text{S}_4$  performed better, possibly because the sea urchin-like structure with a higher specific surface area gained more active sites, shortened the transport length of ions and electrons, and had a larger discharge product space. Furthermore, Wu *et al.* synthesized the spinel catalyst containing  $\text{NiCu}_2\text{S}_4$  and  $\text{CuCo}_2\text{S}_4$  through a method of solvent-thermal reaction, calcination, and subsequent vulcanization<sup>[115]</sup>. The catalysts presented a low voltage gap of 0.73 V between the ORR and OER in a KOH electrolyte, which indicated their potential application in Mg-air batteries.

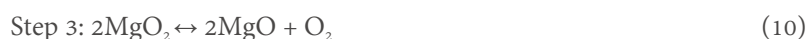
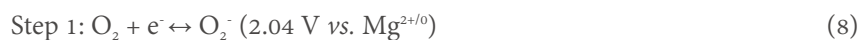
The discharge products ( $\text{MgO}$  and/or  $\text{MgO}_2$ ) of rechargeable Mg-air batteries are both poor conductors of electrons and insoluble in the electrolyte, resulting in the formation of a passivation layer on the cathode surface. During the charge process, those discharge products directly contacting the active sites can be decomposed, while the other ones cannot, leading to poor overall catalytic performance. By comparison, liquid-phase RM bifunctional catalysts can enter the pores of the electrode with the help of the electrolyte and catalyze the cathodic reactions efficiently. However, few studies have been reported on the liquid-phase RM bifunctional catalysts for rechargeable Mg-air batteries, while the researchers mainly concentrated on rechargeable Li-air batteries. Sun *et al.* reported that the soluble iron phthalocyanine ( $\text{FePc}$ ) could catalyze both the ORR and OER processes<sup>[116]</sup>. The RM catalyst acted as an electronic transport mediator between the electrode and lithium peroxide to reduce the overpotential during the charge process, while it also combined with superoxide ions to promote the growth of lithium peroxide during the discharge process, as illustrated in Figure 9E and F. With the help of the stable RM catalyst, the Li-air batteries performed well including more than 130 cycles (limited capacity:  $1000 \text{ mAh}\cdot\text{g}^{-1}$ ) at the current density of  $0.5 \text{ mA}\cdot\text{cm}^{-2}$ , negligible discharging potential decay of 0.02 V, and the stable charging potential after 50 cycles. Deng *et al.* added a RM catalyst  $\text{CuCl}_2$  to the electrolyte in Li-air batteries<sup>[117]</sup>. During the initial discharge process, the  $\text{Cu}^{2+}$  was preferentially reduced to the primary reduced form  $\text{Cu}^+$ . Then the  $\text{Cu}^+$  was further reduced to  $\text{Cu}^0$ , and the newly generated Cu chemically reacted with  $\text{O}_2$  and  $\text{Li}^+$ , transforming into  $\text{Cu}^+$  and  $\text{Li}_2\text{O}_2$ . Thus, the  $\text{Cu}^0/\text{Cu}^+$  redox couple effectively served as the ORR process RM catalyst. During the charge process, the  $\text{Cu}^+$  was firstly oxidized to  $\text{Cu}^{2+}$ , which chemically decomposed  $\text{Li}_2\text{O}_2$  and turned back to  $\text{Cu}^+$ , and therefore the  $\text{Cu}^{2+}/\text{Cu}^+$  redox couple performed as the OER process RM catalyst [Figure 9G]. Eventually, thanks to the  $\text{Cu}^+/\text{Cu}^{2+}$  redox couple, the charge potential was reduced to 3.5 V, and the  $\text{Cu}^+/\text{Cu}^0$  redox couple helped to realize the specific capacity of  $14,700 \text{ mAh}\cdot\text{g}^{-1}$  and also inhibited the superoxidation reaction to stabilize the discharging process.

### Cathodic discharge products of rechargeable Mg-air batteries

So far, researchers have not developed a deep understanding of the reaction mechanism of charge and discharge processes for Mg-air batteries. The example of the Na- $\text{O}_2$  system has shown that the properties of the discharge products (typically a metal oxide, peroxide, or superoxide) can strongly impact the overall energy density<sup>[118]</sup>. Therefore, analyzing the discharge products for rechargeable Mg-air batteries is of great

research significance.

As we have discussed, the reason for the irreversibility of aqueous Mg-air batteries can be accounted for the potential necessary for recharging leading to the decomposition of water solvent. In nonaqueous electrolytes, using RMs is one solution to make Mg-air batteries rechargeable<sup>[13-15]</sup>. In 2015, Vardar *et al.* reported a new rechargeable room-temperature Mg-O<sub>2</sub> battery without RMs<sup>[12]</sup>. The constructed Mg-O<sub>2</sub> cell with (PhMgCl)<sub>4</sub>-Al(OPh)<sub>3</sub>/THF electrolyte could be run for three cycles at room temperature [Figure 10A], and the energy efficiency for the first cycle is 42%, comparable to those for elevated-temperature Mg-O<sub>2</sub> cells. The composition of discharge products was observed to be roughly 70% MgO and 30% amorphous Mg O<sub>2</sub> on a volumetric basis. Vardar *et al.* used the ECC (“electrochemical-chemical-chemical”) mechanism to claim the reaction pathways<sup>[12]</sup>:



During the charge process, MgO<sub>2</sub> decomposed first, followed by more limited MgO decomposition. The low energy efficiency and the capacity loss could be attributed to the incomplete decomposition of discharge products [Figure 10B].

In 2016, Smith *et al.* further studied the electrochemical processes on the surfaces of possible discharge products (MgO and MgO<sub>2</sub>) through DFT calculations and the results showed that pathways involving oxygen intermediates were preferred<sup>[16]</sup>. They pointed out that even though the maximum energy density could be achieved when MgO served as the discharge product, the surface-mediated reactions should be avoided due to its inefficiency. Moreover, the batteries that generate magnesium oxide were less efficient on the round-trip efficiency, while those that generate magnesium peroxide were more efficient (90%) [Figure 10C] because there was a lower overpotential, which was consistent with the experimental results<sup>[12]</sup>. Therefore, either choosing a solution-phase way rather than a surface-mediated way to form MgO or controlling the discharge product by forming MgO<sub>2</sub> is an efficient way to acquire a well-performing rechargeable Mg-air battery. In 2018, Bhauriyal *et al.* studied the issue of the initial nucleation reactions on the surface of catalytic cathodes using DFT calculations<sup>[19]</sup>. They used the calculated free energy diagrams for the redox reactions of oxygen to identify the rate-determining step controlling the overpotentials for the initial nucleation of MgO and MgO<sub>2</sub>. It was indicated that the overpotential of the controlling steps for MgO<sub>2</sub> nucleation is comparatively less than that of MgO formation. Moreover, the preferable formation of MgO<sub>2</sub> cluster compared to MgO on the graphene surface was revealed by ab initio molecular dynamic simulation (AIMD), and this result further confirmed the selectivity of MgO<sub>2</sub> formation over MgO as the final discharge product.

It was indicated that the performance of rechargeable Mg-O<sub>2</sub> batteries could be optimized via cathode designs and operating scenarios that favored the formation of MgO<sub>2</sub> discharge product through multistep pathways involving intermediates, less-reduced species.

Although theoretical and experimental investigations on air cathode reactions have demonstrated promising results, further research is still needed to develop Mg-air batteries with good cycling performance. Here, we present our perspectives that might be helpful for designing promising RMs in

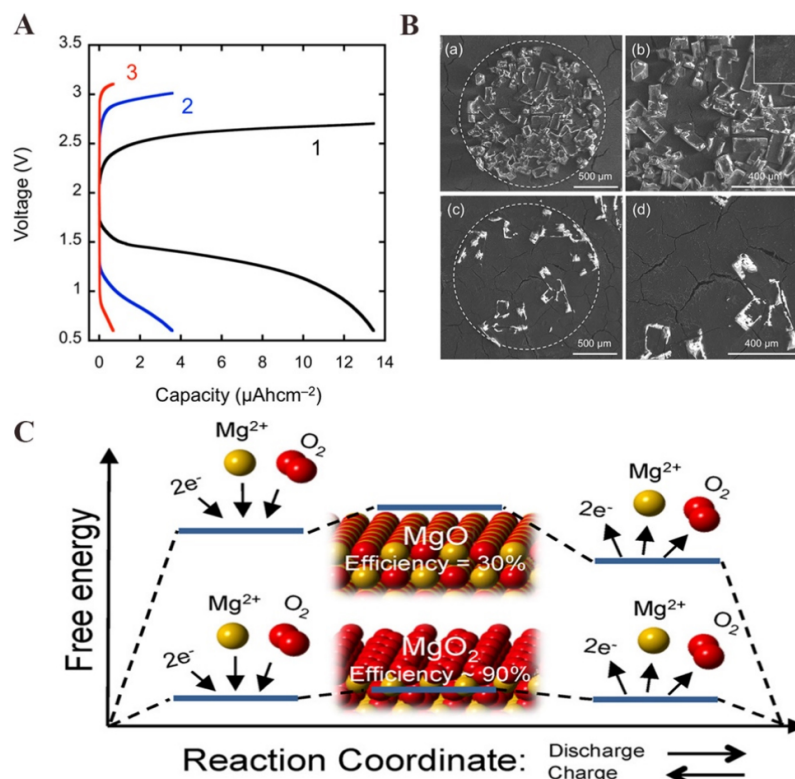


**Figure 10.** (A) Discharge/charge profiles of Mg-air batteries in  $(\text{PhMgCl})_4\text{-Al(OPh)}_3/\text{THF}$  electrolyte under  $25^\circ\text{C}$ <sup>[12]</sup>. (B) SEM images of first discharge products (a), higher magnification of the first discharge products (b) and SEM images of the air electrode after its first charge process (c), higher magnification of the residual product after the first charge process (d)<sup>[12]</sup>. (C) Calculated free energy diagram of different reaction paths of Mg-air batteries<sup>[16]</sup>. Reproduced from Refs.<sup>[12,16]</sup> with permission from the American Chemical Society.

future rechargeable Mg-air batteries:

(1) It is effective to design multivalent compounds that can form different reversible redox couples. Compounds are first reduced to a lower valence state and oxidized to a middle oxidized state to catalyze the ORR process, while also be oxidized first to a higher valence state and reduced to a middle oxidized state to catalyze the OER process.

(2) The formation of superoxides severely decreases the discharge potential of rechargeable batteries, deactivates the catalytic core in cathodes, and decomposes the electrolyte contacting the cathode side, so it is worth more efforts to research how to dodge the formation of magnesium superoxides under the application of RMs.

(3) Except for taking the role of RMs, one effective way to facilitate the OER process is to transform the residual discharge products. It is practical to use additives that can turn discharge products ( $\text{MgO}$  and  $\text{MgO}_2$ ) into compounds with higher ionic and electronic conductivity.

(4) As for the practical molecular design, the steric hindrance around the redox core should be taken into consideration. It is widely believed that exposure to redox core positively impacts the catalytic effect<sup>[120]</sup>.

There is a growing body of literature that recognizes the importance of studying the discharge mechanism of rechargeable Mg-air batteries. It is greatly recommended to combine various advanced characterization technologies (e.g., *in situ* analyses, differential electrochemical mass spectrometry, and so on) with theoretical calculations to gain insights into the electrochemical processes and address the unsolved scientific problems.

## THEORETICAL CALCULATIONS

With the development of computational simulation technologies, theoretical calculations have developed rapidly in recent years, providing an effective method for researchers to understand the complicated systems in batteries. Using quantum computing techniques like DFT and finite element simulations, molecular dynamics simulates the motions of particles through mathematics, physics, and chemistry, which support the calculation of the forces and energies under different interactions<sup>[121]</sup>. The properties of the electrochemical materials, such as structures, reaction activity, and stability, can be presented by theoretical calculations<sup>[122]</sup>. For rechargeable Mg-air batteries, such techniques can not only be used for validation of reaction pathways and mechanisms of the ORR and OER processes, but also for feasibility analysis of the material candidates, including anodes, cathodes, and electrolytes, before being applied to experiments.

Passivation is the crucial factor limiting the electrochemical properties of Mg anodes. Based on first-principles calculations and ion-transport theory, Chen *et al.* systematically studied a variety of compounds as potential coating materials for a Mg metal anode<sup>[123,124]</sup>. In addition, DFT studies can also investigate the reaction pathway, activity, and stability of different pure and alloyed metals, and the properties of the electrode/electrolyte interface<sup>[125]</sup>.

A suitable electrolyte is crucial for Mg-air battery performance. In the past few years, theoretical calculations have been widely used in Mg battery electrolytes to gain insights into the transport behavior of Mg ions and their plating/stripping mechanisms at the electrolyte/electrode interface<sup>[126-128]</sup>. First-principles molecular dynamics simulations can be used to obtain the electrochemical stability window, solvation energy, decomposition path of electrolytes and their correlation with the intermolecular interactions and the resulting speciation of the Mg<sup>2+</sup><sup>[125-128]</sup>.

Developing catalysts is typically expensive and time-consuming, and the components of bifunctional air catalysts typically include noble or toxic metals (i.e., Pt, Ag, and Co)<sup>[126]</sup>. Modeling and calculation can predict the experimental results and guide the experiments effectively. Previous studies have been conducted to model and calculate the cathode discharge reaction paths<sup>[120]</sup>, initial nucleation of discharge products (MgO and MgO<sub>2</sub>)<sup>[16]</sup>, and their equilibrium conductivity associated with the intrinsic ionic (point) defects<sup>[17]</sup>. Furthermore, DFT studies can calculate the composition and electronic conductivity of passivation film on the cathodes and predict the catalytic activity towards the ORR and OER of activity sites on the catalyst surface<sup>[129]</sup>. Moreover, DFT calculations can be used to acquire the molecular properties such as molecular orbital energy levels, reaction Gibbs free energy, binding energy with O<sub>2</sub> molecules, and molecular bond energy of RMs<sup>[130,131]</sup>, which helps to demonstrate the catalytic mechanism and design the molecular structures of RMs that can be used in future Mg-air batteries.

## APPLICATIONS

Mg-air batteries have large specific energy, no environmental pollution, and higher theoretical capacity density than those traditional batteries such as lithium batteries, lead-acid batteries, and so on. At present, aqueous Mg-air batteries can achieve a high service life by replacing the anode. Based on the above advantages, primary Mg-air batteries can be used as a power source for military and vehicles. In 1996,

Norway and Italy jointly developed magnesium fuel cells and applied them to the marine underwater automatic control system for the detection of submarine oil or gas wells at a depth of 180 m. The seawater battery was based on commercial Mg alloy as the anode and dissolved oxygen in the seawater as the oxidant in the seawater electrolyte. This battery system had an energy of 650 kWh and was designed for a life of 15 years<sup>[132]</sup>.

Mg-air batteries are also considered a backup power source that can be put into use after adding electrolytes while left dry for a long time during backup. The 100 W and 300 W magnesium/brine/air fuel cells (MASWFCs) developed by Greenvolt Power in Canada had an energy density of more than 20 times that of lead-acid batteries, and can power TVs, lights, portable computers, mobile phones, and GPS equipment. The brine electrolyte magnesium/air fuel cell developed by MagPower Systems in Canada could continuously provide 300 W of power and had been successfully applied to the power supply of water purification system pumps in remote areas<sup>[133]</sup>.

Furthermore, Mg-air batteries are biocompatible as Mg<sup>2+</sup> ions show no toxicity towards the environment and the human body. Mg-air batteries can be made into a fiber shape with high flexibility by material design. Cheng *et al.* fabricated an atomic Fe-N<sub>x</sub> coupled open-mesoporous N-doped-carbon nanofiber electrodes as Mg-air battery cathodes<sup>[134]</sup>. The Mg-air batteries with the fiber-shaped electrodes revealed high capacity, long operating life, and good flexibility. In addition, the Mg-air battery with dual-layer gel electrolyte<sup>[55]</sup> could also be made into a flexible fiber shape with a coaxial structure, and it exhibited a stable voltage after bending to 45°, 90°, and 135°. This property presents a huge opportunity for the next generation of wearable and biocompatible power supplies.

## CONCLUSION AND OUTLOOK

The Mg-air battery technology is still in its early development stage. In this review, we have summarized the role of various components of Mg-air batteries (anode, electrolyte, and cathode) in battery performance and recent research advances. The primary problems of Mg anode are the high level of corrosion in aqueous electrolytes and low Coulombic efficiency in organic electrolytes. Nanostructured Mg and Mg alloys containing high hydrogen evolution overpotential elements along with protective layers are promising to suppress corrosion and improve the performance of Mg anode. Meanwhile, designing an effective modification layer on the Mg anode may largely improve the battery performance by increasing the Mg<sup>2+</sup> Faradaic efficiency and discharge voltage, as well as improving the tolerance to H<sub>2</sub>O and CO<sub>2</sub> from the air. The sluggish kinetics of the ORR on the air cathodes is another obstacle hindering the discharge properties of primary Mg-air batteries. Noble metal materials, transition metal oxides, nitrogen-containing metal macrocycles, and carbon-based materials are the four types of mainly used catalysts for primary Mg-air batteries. More efforts on low cost, high activity, and durability catalyst substitutes for noble metals are necessary. The electrolyte plays a crucial role in improving the performance of the Mg-air batteries. The current problems of aqueous electrolytes focus on low Mg utilization and poor discharge voltage. Additives that can decrease the corrosion rate and improve electrochemical properties of batteries simultaneously are still upon further development. For nonaqueous electrolytes, it is necessary to seek new systems ensuring Mg plating/stripping with low overpotentials under the O<sub>2</sub> atmosphere and supporting the decomposition of discharge products. Furthermore, the flexible design of gel electrolytes is a new direction for wearable and biocompatible Mg-air batteries.

At present, the aqueous electrolytes are commonly used in primary Mg-air batteries which can obtain a long service life by replacing the exhausted Mg anodes. However, aqueous Mg-air batteries are irreversible as the result of the formation of a magnesium hydroxide passivation layer that cannot be decomposed in moderate

voltage ranges. Optimizing the composition of the electrolytes can reduce the corrosion rate of Mg anodes and simultaneously pave the way for rechargeable Mg-air batteries.

For rechargeable Mg-air batteries, the key solution to achieving reversibility is to introduce RMs to the battery system to reduce the reaction barrier and develop bifunctional catalysts that are active for both ORR and OER. Furthermore, it has been proven by theoretical calculations and experimental results that the discharge reaction favoring the formation of  $\text{MgO}_2$  is more likely to be recharged with a higher voltage efficiency than that favoring the formation of  $\text{MgO}$ . The electrolytes for rechargeable Mg-air batteries should support the reversible Mg plating/stripping on the anode side and reversible ORR/OER on the cathode side simultaneously, as well as contain low viscosity, low volatility, wide electrochemical window, and high ionic conductivity. Moreover, gel-polymer electrolytes and ionic liquid electrolytes can be excellent candidates for rechargeable Mg-air batteries while also deserve embedded research. Especially, updated strategies and formulas of the electrolytes for rechargeable Mg metal batteries are strongly recommended to apply in rechargeable Mg-air batteries.

In general, Mg-air batteries present high theoretical specific energy and energy density, so they contain great research value. However, there is still a long way to achieve the rechargeability of Mg-air battery system, and it is essential to conduct deep theoretical research and more *in situ* analyses, especially the stable nonaqueous electrolytes and excellent bifunctional catalysts.

## DECLARATIONS

### Authors' contributions

Conceptualization, data curation, writing - original draft: Wang Y, Sun Y

Data curation, formal analysis: Ren W, Zhang D

Validation, formal analysis: Yang Y

Supervision: Yang J, Wang J

Supervision, writing - review and editing: NuLi Y, Zeng X

### Availability of data and materials

Not applicable.

### Financial support and sponsorship

This work was supported by the Oceanic Interdisciplinary Program of Shanghai Jiao Tong University (No. WH410260401/006), National Natural Science Foundation of China (No. 21975159, 21573146, U1705255) and Shanghai Aerospace Science and Technology Innovation Fund (No. SAST2018-117).

### Conflicts of interest

All authors declared that there are no conflicts of interest.

### Ethical approval and consent to participate

Not applicable.

### Consent for publication

Not applicable.

### Copyright

© The Author(s) 2022.

## REFERENCES

1. He G, Ciez R, Moutis P, Kar S, Whitacre JF. The economic end of life of electrochemical energy storage. *Appl Energy* 2020;273:115151. DOI
2. Paul S. Materials and electrochemistry: present and future battery. *J Electrochem Sci Technol* 2016;7:115-31. DOI
3. Wagner FT, Lakshmanan B, Mathias MF. Electrochemistry and the future of the automobile. *J Phys Chem Lett* 2010;1:2204-19. DOI
4. Kwak WJ, Rosy, Sharon D, et al. Lithium-oxygen batteries and related systems: potential, status, and future. *Chem Rev* 2020;120:6626-83. DOI PubMed
5. Li H, Ma L, Han C, et al. Advanced rechargeable zinc-based batteries: recent progress and future perspectives. *Nano Energy* 2019;62:550-87. DOI
6. Liu Y, Sun Q, Li W, Adair KR, Li J, Sun X. A comprehensive review on recent progress in aluminum-air batteries. *Green Energy Environ* 2017;2:246-77. DOI
7. Zhang T, Tao Z, Chen J. Magnesium-air batteries: from principle to application. *Mater Horiz* 2014;1:196-206. DOI
8. Li C, Sun Y, Gebert F, Chou S. Current progress on rechargeable magnesium-air battery. *Adv Energy Mater* 2017;7:1700869. DOI
9. Rahman MA, Wang X, Wen C. High energy density metal-air batteries: a review. *J Electrochem Soc* 2013;160:A1759-71. DOI
10. Wang H, Ryu J, Shao Y, et al. Advancing electrolyte solution chemistry and interfacial electrochemistry of divalent metal batteries. *ChemElectroChem* 2021;8:3013-29. DOI
11. Mu T, Zhang J, Shi R, et al. Ultrahigh rate capability and long cycling stability of dual-ion batteries enabled by TiO<sub>2</sub> microspheres with abundant oxygen vacancies. *Chem Commun* 2020;56:8039-42. DOI PubMed
12. Vardar G, Nelson EG, Smith JG, et al. Identifying the discharge product and reaction pathway for a secondary Mg/O<sub>2</sub> battery. *Chem Mater* 2015;27:7564-8. DOI
13. Shiga T, Hase Y, Kato Y, Inoue M, Takechi K. A rechargeable non-aqueous Mg-O<sub>2</sub> battery. *Chem Commun* 2013;49:9152-4. DOI PubMed
14. Shiga T, Hase Y, Yagi Y, Takahashi N, Takechi K. Catalytic cycle employing a TEMPO-anion complex to obtain a secondary Mg-O<sub>2</sub> battery. *J Phys Chem Lett* 2014;5:1648-52. DOI PubMed
15. Dong Q, Yao X, Luo J, Zhang X, Hwang H, Wang D. Enabling rechargeable non-aqueous Mg-O<sub>2</sub> battery operations with dual redox mediators. *Chem Commun* 2016;52:13753-6. DOI PubMed
16. Smith JG, Naruse J, Hiramatsu H, Siegel DJ. Theoretical limiting potentials in Mg/O<sub>2</sub> Batteries. *Chem Mater* 2016;28:1390-401. DOI
17. Smith JG, Naruse J, Hiramatsu H, Siegel DJ. Intrinsic conductivity in magnesium-oxygen battery discharge products: MgO and MgO<sub>2</sub>. *Chem Mater* 2017;29:3152-63. DOI
18. Chen X, Liu X, Le Q, Zhang M, Liu M, Atrens A. A comprehensive review of the development of magnesium anodes for primary batteries. *J Mater Chem A* 2021;9:12367-99. DOI
19. Li W, Li C, Zhou C, Ma H, Chen J. Metallic magnesium nano/mesoscale structures: their shape-controlled preparation and mg/air battery applications. *Angew Chem Int Ed* 2006;45:6009-12. DOI PubMed
20. Xin G, Wang X, Wang C, Zheng J, Li X. Porous Mg thin films for Mg-air batteries. *Dalton Trans* 2013;42:16693-6. DOI PubMed
21. Zhao Y, Du A, Dong S, et al. A bismuth-based protective layer for magnesium metal anode in noncorrosive electrolytes. *ACS Energy Lett* 2021;6:2594-601. DOI
22. Gu X, Zheng Y, Cheng Y, Zhong S, Xi T. In vitro corrosion and biocompatibility of binary magnesium alloys. *Biomaterials* 2009;30:484-98. DOI PubMed
23. Deng M, Höche D, Lamaka SV, Snihirova D, Zheludkevich ML. Mg-Ca binary alloys as anodes for primary Mg-air batteries. *J Power Sources* 2018;396:109-18. DOI
24. Ma J, Wang G, Li Y, Qin C, Ren F. Electrochemical investigations on AZ series magnesium alloys as anode materials in a sodium chloride solution. *J Mater Eng Perform* 2019;28:2873-80. DOI
25. Ma J, Wang G, Li Y, Ren F, Volinsky AA. Electrochemical performance of Li Mg-air batteries based on AZ series magnesium alloys. *Ionics* 2019;25:2201-9. DOI
26. Wang N, Mu Y, Xiong W, Zhang J, Li Q, Shi Z. Effect of crystallographic orientation on the discharge and corrosion behaviour of AP65 magnesium alloy anodes. *Corrosion Science* 2018;144:107-26. DOI
27. Zhao J, Yu K, Hu Y, et al. Discharge behavior of Mg-4wt%Ga-2wt%Hg alloy as anode for seawater activated battery. *Electrochim Acta* 2011;56:8224-31. DOI
28. Yuasa M, Huang X, Suzuki K, Mabuchi M, Chino Y. Discharge properties of Mg-Al-Mn-Ca and Mg-Al-Mn alloys as anode materials for primary magnesium-air batteries. *J Power Sources* 2015;297:449-56. DOI
29. Wang N, Wang R, Peng C, Feng Y, Zhang X. Influence of aluminium and lead on activation of magnesium as anode. *T Nonferr Metal Soc* 2010;20:1403-11. DOI
30. Liu X, Xue J, Liu S. Discharge and corrosion behaviors of the  $\alpha$ -Mg and  $\beta$ -Li based Mg alloys for Mg-air batteries at different current densities. *Mater Des* 2018;160:138-46. DOI
31. Sivashanmugam A, Prem kumar T, Renganathan NG, Gopukumar S. Performance of a magnesium-lithium alloy as an anode for magnesium batteries. *J Appl Electrochem* 2004;34:1135-9. DOI
32. Gusieva K, Davies CHJ, Scully JR, Birbilis N. Corrosion of magnesium alloys: the role of alloying. *Int Mater Rev* 2014;60:169-94.

DOI

33. Ma Y, Li N, Li D, Zhang M, Huang X. Performance of Mg-14Li-1Al-0.1Ce as anode for Mg-air battery. *J Power Sources* 2011;196:2346-50. DOI
34. Wang N, Wang R, Peng C, Peng B, Feng Y, Hu C. Discharge behaviour of Mg-Al-Pb and Mg-Al-Pb-In alloys as anodes for Mg-air battery. *Electrochim Acta* 2014;149:193-205. DOI
35. Liu X, Liu S, Xue J. Discharge performance of the magnesium anodes with different phase constitutions for Mg-air batteries. *J Power Sources* 2018;396:667-74. DOI
36. Zheng T, Hu Y, Zhang Y, Yang S, Pan F. Composition optimization and electrochemical properties of Mg-Al-Sn-Mn alloy anode for Mg-air batteries. *Mater Des* 2018;137:245-55. DOI
37. Xiong H, Yu K, Yin X, Dai Y, Yan Y, Zhu H. Effects of microstructure on the electrochemical discharge behavior of Mg-6wt%Al-1wt%Sn alloy as anode for Mg-air primary battery. *J Alloys Compd* 2017;708:652-61. DOI
38. Yuasa M, Huang X, Suzuki K, Mabuchi M, Chino Y. Effects of microstructure on discharge behavior of AZ91 alloy as anode for Mg-air battery. *Mater Trans* 2014;55:1202-7. DOI
39. Hoey GR, Cohen M. Corrosion of anodically and cathodically polarized magnesium in aqueous media. *J Electrochem Soc* 1958;105:245. DOI
40. Song G, Atrens A, Stjohn D, Nairn J, Li Y. The electrochemical corrosion of pure magnesium in 1 N NaCl. *Corros Sci* 1997;39:855-75. DOI
41. Birbilis N, King A, Thomas S, Frankel G, Scully J. Evidence for enhanced catalytic activity of magnesium arising from anodic dissolution. *Electrochim Acta* 2014;132:277-83. DOI
42. Lebouil S, Duboin A, Monti F, Tabeling P, Volovitch P, Ogle K. A novel approach to on-line measurement of gas evolution kinetics: application to the negative difference effect of Mg in chloride solution. *Electrochim Acta* 2014;124:176-82. DOI
43. Song G, Atrens A. Understanding magnesium corrosion—a framework for improved alloy performance. *Adv Eng Mater* 2003;5:837-58. DOI
44. Richey FW, McCloskey BD, Luntz AC. Mg anode corrosion in aqueous electrolytes and implications for Mg-air batteries. *J Electrochem Soc* 2016;163:A958-63. DOI
45. Shrestha N, Raja KS, Utgikar V. Mg-RE alloy anode materials for Mg-air battery application. *J Electrochem Soc* 2019;166:A3139-53. DOI
46. Sathyanarayana S, Munichandraiah N. A new magnesium - air cell for long-life applications. *J Appl Electrochem* 1981;11:33-9. DOI
47. Deyab M. Decyl glucoside as a corrosion inhibitor for magnesium-air battery. *J Power Sources* 2016;325:98-103. DOI
48. Vaghefinazari B, Höche D, Lamaka SV, Snihirova D, Zheludkevich ML. Tailoring the Mg-air primary battery performance using strong complexing agents as electrolyte additives. *J Power Sources* 2020;453:227880. DOI
49. Dinesh M, Saminathan K, Selvam M, Srithar S, Rajendran V, Kaler KV. Water soluble graphene as electrolyte additive in magnesium-air battery system. *J Power Sources* 2015;276:32-8. DOI
50. Liu J, Xu C, Chen Z, Ni S, Shen ZX. Progress in aqueous rechargeable batteries. *Green Energy Environ* 2018;3:20-41. DOI
51. Lu Z, Schechter A, Moshkovich M, Aurbach D. On the electrochemical behavior of magnesium electrodes in polar aprotic electrolyte solutions. *J Electroanal Chem* 1999;466:203-17. DOI
52. Vardar G, Smith JG, Thompson T, et al. Mg/O<sub>2</sub> Battery based on the magnesium–aluminum chloride complex (MACC) electrolyte. *Chem Mater* 2016;28:7629-37. DOI
53. Yi J, Liu X, Guo S, Zhu K, Xue H, Zhou H. Novel stable gel polymer electrolyte: toward a high safety and long life Li-air battery. *ACS Appl Mater Interfaces* 2015;7:23798-804. DOI PubMed
54. Liew SY, Juan JC, Lai CW, Pan G, Yang TC, Lee TK. An eco-friendly water-soluble graphene-incorporated agar gel electrolyte for magnesium-air batteries. *Ionics* 2019;25:1291-301. DOI
55. Li L, Chen H, He E, et al. High-energy-density magnesium-air battery based on dual-layer gel electrolyte. *Angew Chem Int Ed* 2021;60:15317-22. DOI PubMed
56. Armand M, Endres F, MacFarlane DR, Ohno H, Scrosati B. Ionic-liquid materials for the electrochemical challenges of the future. *Nat Mater* 2009;8:621-9. DOI PubMed
57. Galiński M, Lewandowski A, Stępniański I. Ionic liquids as electrolytes. *Electrochim Acta* 2006;51:5567-80. DOI
58. MacFarlane DR, Forsyth M, Howlett PC, et al. Ionic liquids and their solid-state analogues as materials for energy generation and storage. *Nat Rev Mater* 2016;1:15005. DOI
59. Han L, Lehmann ML, Zhu J, et al. Recent developments and challenges in hybrid solid electrolytes for lithium-ion batteries. *Front Energy Res* 2020;8:202. DOI
60. Karuppasamy K, Theerthagiri J, Vikraman D, et al. Ionic liquid-based electrolytes for energy storage devices: a brief review on their limits and applications. *Polymers* 2020;12:918. DOI PubMed PMC
61. Åvall G, Mindemark J, Brandell D, Johansson P. Sodium-ion battery electrolytes: modeling and simulations. *Adv Energy Mater* 2018;8:1703036. DOI
62. Saha P, Datta MK, Velikokhatnyi OI, Manivannan A, Alman D, Kumta PN. Rechargeable magnesium battery: current status and key challenges for the future. *Prog Mater Sci* 2014;66:1-86. DOI
63. Mandai T, Dokko K, Watanabe M. Solvate ionic liquids for Li, Na, K, and Mg batteries. *Chem Rec* 2018;19:708-22. DOI PubMed
64. Fu J, Cano ZP, Park MG, Yu A, Fowler M, Chen Z. Electrically rechargeable zinc-air batteries: progress, challenges, and

- perspectives. *Adv Mater* 2017;29:1604685. DOI PubMed
65. Kang Y, Liang F, Hayashi K. Hybrid sodium-air cell with Na[FSA-C2C1im][FSA] ionic liquid electrolyte. *Electrochim Acta* 2016;218:119-24. DOI
  66. Xie J, Zhang Q. Recent progress in multivalent metal (Mg, Zn, Ca, and Al) and metal-ion rechargeable batteries with organic materials as promising electrodes. *Small* 2019;15:e1805061. DOI PubMed
  67. Dokko K, Tachikawa N, Yamauchi K, et al. Solvate ionic liquid electrolyte for Li-S batteries. *J Electrochem Soc* 2013;160:A1304-10. DOI
  68. Li Z, Kamei Y, Haruta M, et al. Si/Li<sub>2</sub>S battery with solvate ionic liquid electrolyte. *Electrochemistry* 2016;84:887-90. DOI
  69. Yan Y, Gunzelmann D, Pozo-gonzalo C, et al. Investigating discharge performance and Mg interphase properties of an Ionic Liquid electrolyte based Mg-air battery. *Electrochim Acta* 2017;235:270-9. DOI
  70. Khoo T, Somers A, Torriero AA, Macfarlane DR, Howlett PC, Forsyth M. Discharge behaviour and interfacial properties of a magnesium battery incorporating trihexyl(tetradecyl)phosphonium based ionic liquid electrolytes. *Electrochim Acta* 2013;87:701-8. DOI
  71. Zhu N, Zhang K, Wu F, Bai Y, Wu C. Ionic liquid-based electrolytes for aluminum/magnesium/sodium-ion batteries. *Energy Mater Adv* 2021;2021:1-29. DOI
  72. Kar M, Ma Z, Azofra LM, Chen K, Forsyth M, MacFarlane DR. Ionic liquid electrolytes for reversible magnesium electrochemistry. *Chem Commun* 2016;52:4033-6. DOI PubMed
  73. Su S, Nuli Y, Wang N, Yusipu D, Yang J, Wang J. Magnesium borohydride-based electrolytes containing 1-butyl-1-methylpiperidinium bis(trifluoromethyl sulfonyl)imide ionic liquid for rechargeable magnesium batteries. *J Electrochem Soc* 2016;163:D682-8. DOI
  74. Gao X, Mariani A, Jeong S, et al. Prototype rechargeable magnesium batteries using ionic liquid electrolytes. *J Power Sources* 2019;423:52-9. DOI
  75. Law Y, Schnaidt J, Brimaud S, Behm R. Oxygen reduction and evolution in an ionic liquid ([BMP][TFSA]) based electrolyte: a model study of the cathode reactions in Mg-air batteries. *J Power Sources* 2016;333:173-83. DOI
  76. Bozorgchenani M, Fischer P, Schnaidt J, et al. Electrocatalytic oxygen reduction and oxygen evolution in Mg-free and Mg-containing ionic liquid 1-Butyl-1-Methylpyrrolidinium Bis (Trifluoromethanesulfonyl) imide. *ChemElectroChem* 2018;5:2600-11. DOI
  77. Jusys Z, Schnaidt J, Behm RJ. O<sub>2</sub> reduction on a Au film electrode in an ionic liquid in the absence and presence of Mg<sup>2+</sup> ions: product formation and adlayer dynamics. *J Chem Phys* 2019;150:041724. DOI PubMed
  78. Nørskov JK, Rossmeisl J, Logadottir A, et al. Origin of the overpotential for oxygen reduction at a fuel-cell cathode. *J Phys Chem B* 2004;108:17886-92. DOI
  79. Huang Z, Wang J, Peng Y, Jung C, Fisher A, Wang X. Design of efficient bifunctional oxygen reduction/evolution electrocatalyst: recent advances and perspectives. *Adv Energy Mater* 2017;7:1700544. DOI
  80. Gasteiger HA, Kocha SS, Sompalli B, Wagner FT. Activity benchmarks and requirements for Pt, Pt-alloy, and non-Pt oxygen reduction catalysts for PEMFCs. *Appl Catal B* 2005;56:9-35. DOI
  81. Cheng F, Chen J. Metal-air batteries: from oxygen reduction electrochemistry to cathode catalysts. *Chem Soc Rev* 2012;41:2172-92. DOI PubMed
  82. Perez J, Gonzalez E, Ticianelli E. Oxygen electrocatalysis on thin porous coating rotating platinum electrodes. *Electrochim Acta* 1998;44:1329-39. DOI
  83. Huang Q, Yang H, Tang Y, Lu T, Akins DL. Carbon-supported Pt-Co alloy nanoparticles for oxygen reduction reaction. *Electrochem Commun* 2006;8:1220-4. DOI
  84. Chen C, Kang Y, Huo Z, et al. Highly crystalline multimetallic nanoframes with three-dimensional electrocatalytic surfaces. *Science* 2014;343:1339-43. DOI PubMed
  85. Zhao Y, Wu Y, Liu J, Wang F. Dependent relationship between quantitative lattice contraction and enhanced oxygen reduction activity over Pt-Cu alloy catalysts. *ACS Appl Mater Interfaces* 2017;9:35740-8. DOI PubMed
  86. Jong Yoo S, Kim SK, Jeon TY, et al. Enhanced stability and activity of Pt-Y alloy catalysts for electrocatalytic oxygen reduction. *Chem Commun* 2011;47:11414-6. DOI PubMed
  87. Gao J, Zou J, Zeng X, Ding W. Carbon supported nano Pt-Mo alloy catalysts for oxygen reduction in magnesium-air batteries. *RSC Adv* 2016;6:83025-30. DOI
  88. Qaseem A, Chen F, Wu X, Johnston RL. Pt-free silver nanoalloy electrocatalysts for oxygen reduction reaction in alkaline media. *Catal Sci Technol* 2016;6:3317-40. DOI
  89. Kukunuri S, Naik K, Sampath S. Effects of composition and nanostructuring of palladium selenide phases, Pd<sub>4</sub>Se, Pd<sub>7</sub>Se<sub>4</sub> and Pd<sub>17</sub>Se<sub>15</sub>, on ORR activity and their use in Mg-air batteries. *J Mater Chem A* 2017;5:4660-70. DOI
  90. Outiki O, Lamy-pitara E, Barbier J. Platinum-palladium catalysts for fuel cell oxygen electrodes. *React Kinet Catal Lett* 1983;23:213-20. DOI
  91. Burke LD, Casey JK. An examination of the electrochemical behavior of palladium electrodes in acid. *J Electrochem Soc* 1993;140:1284-91. DOI
  92. Jiang L, Hsu A, Chu D, Chen R. Oxygen reduction reaction on carbon supported Pt and Pd in alkaline solutions. *J Electrochem Soc* 2009;156:B370. DOI
  93. Cao Y, Yang H, Ai X, Xiao L. The mechanism of oxygen reduction on MnO<sub>2</sub>-catalyzed air cathode in alkaline solution. *J Electroanal*

- Chem* 2003;557:127-34. DOI
94. Li CS, Sun Y, Lai WH, Wang JZ, Chou SL. Ultrafine Mn<sub>3</sub>O<sub>4</sub> nanowires/three-dimensional graphene/single-walled carbon nanotube composites: superior electrocatalysts for oxygen reduction and enhanced Mg/air batteries. *ACS Appl Mater Interfaces* 2016;8:27710-9. DOI PubMed
  95. Lambert TN, Vigil JA, White SE, et al. Understanding the effects of cationic dopants on  $\alpha$ -MnO<sub>2</sub> oxygen reduction reaction electrocatalysis. *J Phys Chem C* 2017;121:2789-97. DOI
  96. Davis DJ, Lambert TN, Vigil JA, et al. Role of Cu-ion doping in Cu- $\alpha$ -MnO<sub>2</sub> nanowire electrocatalysts for the oxygen reduction reaction. *J Phys Chem C* 2014;118:17342-50. DOI
  97. Wu KH, Zeng Q, Zhang B, et al. Structural origin of the activity in Mn<sub>3</sub>O<sub>4</sub>-graphene oxide hybrid electrocatalysts for the oxygen reduction reaction. *ChemSusChem* 2015;8:3331-9. DOI PubMed
  98. Boukoureshlieva R, Milusheva Y, Popov I, Trifonova A, Momchilov A. Application of pyrolyzed Cobalt (II) tetramethoxyphenyl porphyrin based catalyst in metal-air systems and enzyme electrodes. *Electrochim Acta* 2020;353:136472. DOI
  99. Liu Y, Zhou G, Zhang Z, et al. Significantly improved electrocatalytic oxygen reduction by an asymmetrical Pacman dinuclear cobalt(ii) porphyrin-porphyrin dyad. *Chem Sci* 2020;11:87-96. DOI PubMed PMC
  100. Huang J, Lu Q, Ma X, Yang X. Bio-inspired FeN<sub>5</sub> moieties anchored on a three-dimensional graphene aerogel to improve oxygen reduction catalytic performance. *J Mater Chem A* 2018;6:18488-97. DOI
  101. Liu H, Song C, Tang Y, Zhang J, Zhang J. High-surface-area CoTMPP/C synthesized by ultrasonic spray pyrolysis for PEM fuel cell electrocatalysts. *Electrochim Acta* 2007;52:4532-8. DOI
  102. Lai L, Potts JR, Zhan D, et al. Exploration of the active center structure of nitrogen-doped graphene-based catalysts for oxygen reduction reaction. *Energy Environ Sci* 2012;5:7936. DOI
  103. Vikkisk M, Kruusenberg I, Joost U, Shulga E, Kink I, Tammeveski K. Electrocatalytic oxygen reduction on nitrogen-doped graphene in alkaline media. *Appl Catal B* 2014;147:369-76. DOI
  104. Liang HW, Zhuang X, Brüller S, Feng X, Müllen K. Hierarchically porous carbons with optimized nitrogen doping as highly active electrocatalysts for oxygen reduction. *Nat Commun* 2014;5:4973. DOI PubMed
  105. Du J, Quinson J, Zhang D, Bizzotto F, Zana A, Arenz M. Bifunctional Pt-IrO<sub>2</sub> catalysts for the oxygen evolution and oxygen reduction reactions: alloy nanoparticles versus nanocomposite catalysts. *ACS Catal* 2021;11:820-8. DOI
  106. Kang Y, Jung SC, Kim H, Han Y, Oh SH. Maximum catalytic activity of Pt<sub>5</sub>M in Li-O<sub>2</sub> batteries: M=group V transition metals. *Nano Energy* 2016;27:1-7. DOI
  107. Li D, Liang J, Robertson SJ, et al. Heterogeneous bimetallic organic coordination polymer-derived Co/Fe@NC bifunctional catalysts for rechargeable Li-O<sub>2</sub> batteries. *ACS Appl Mater Interfaces* 2022;14:5459-67. DOI PubMed
  108. Chen C, Li Y, Cheng D, He H, Zhou K. Graphite nanoarrays-confined Fe and Co single-atoms within graphene sponges as bifunctional oxygen electrocatalyst for ultralong lasting zinc-air battery. *ACS Appl Mater Interfaces* 2020;12:40415-25. DOI PubMed
  109. Xu N, Nie Q, Luo L, et al. Controllable hortensia-like MnO<sub>2</sub> synergized with carbon nanotubes as an efficient electrocatalyst for long-term metal-air batteries. *ACS Appl Mater Interfaces* 2019;11:578-87. DOI PubMed
  110. Débart A, Paterson AJ, Bao J, Bruce PG. Alpha-MnO<sub>2</sub> nanowires: a catalyst for the O<sub>2</sub> electrode in rechargeable lithium batteries. *Angew Chem Int Ed* 2008;47:4521-4. DOI PubMed
  111. Zhu L, Scheiba F, Trouillet V, et al. MnO<sub>2</sub> and reduced graphene oxide as bifunctional electrocatalysts for Li-O<sub>2</sub> batteries. *ACS Appl Energy Mater* 2019;2:7121-31. DOI
  112. Kim K, Kim J. Unique designed structure of bimetallic cobalt and nickel oxide nanocages with nitrogen doping as bifunctional catalysts. *Ionics* 2021;27:845-52. DOI
  113. Fan L; College of Materials Science and Engineering, Heilongjiang Provincial Key Laboratory of Polymeric Composite Materials, Qiqihar University, No.42, Wenhua Street, Qiqihar 161006, PR China. A novel Sm<sub>0.5</sub>Sr<sub>0.5</sub>Co<sub>1-x</sub>Fe<sub>x</sub>O<sub>3- $\delta$</sub> /acetylene black composite as bifunctional electrocatalyst for oxygen reduction/evolution reactions. *Int J Electrochem Sci* 2021;16:210722. DOI
  114. Xu M, Hou X, Yu X, Ma Z, Yang J, Yuan X. Spinel NiCo<sub>2</sub>S<sub>4</sub> as excellent bi-functional cathode catalysts for rechargeable Li-O<sub>2</sub> batteries. *J Electrochem Soc* 2019;166:F406-13. DOI
  115. Wu X, Li S, Liu J, Yu M. Mesoporous hollow nested nanospheres of Ni, Cu, Co-based mixed sulfides for electrocatalytic oxygen reduction and evolution. *ACS Appl Nano Mater* 2019;2:4921-32. DOI
  116. Sun D, Shen Y, Zhang W, et al. A solution-phase bifunctional catalyst for lithium-oxygen batteries. *J Am Chem Soc* 2014;136:8941-6. DOI PubMed
  117. Deng H, Qiao Y, Zhang X, et al. Killing two birds with one stone: a Cu ion redox mediator for a non-aqueous Li-O<sub>2</sub> battery. *J Mater Chem A* 2019;7:17261-5. DOI
  118. Sheng C, Yu F, Wu Y, Peng Z, Chen Y. Disproportionation of sodium superoxide in metal-air batteries. *Angew Chem Int Ed* 2018;57:9906-10. DOI PubMed
  119. Bhauriyal P, Rawat KS, Bhattacharyya G, Garg P, Pathak B. First-principles study of magnesium peroxide nucleation for Mg-air battery. *Chem Asian J* 2018;13:3198-203. DOI PubMed
  120. Kwak W, Park J, Kim H, et al. Oxidation stability of organic redox mediators as mobile catalysts in lithium-oxygen batteries. *ACS Energy Lett* 2020;5:2122-9. DOI
  121. Sun Y, Yang T, Ji H, et al. Boosting the optimization of lithium metal batteries by molecular dynamics simulations: a perspective.

- Adv Energy Mater* 2020;10:2002373. DOI
122. Butler KT, Sai Gautam G, Canepa P. Designing interfaces in energy materials applications with first-principles calculations. *npj Comput Mater* 2019;5:19. DOI
  123. Chen T, Ceder G, Sai Gautam G, Canepa P. Evaluation of Mg compounds as coating materials in Mg batteries. *Front Chem* 2019;7:24. DOI PubMed PMC
  124. Chen T, Sai Gautam G, Canepa P. Ionic transport in potential coating materials for Mg batteries. *Chem Mater* 2019;31:8087-99. DOI
  125. Clark S, Latz A, Horstmann B. A review of model-based design tools for metal-air batteries. *Batteries* 2018;4:5. DOI
  126. Wan LF, Prendergast D. The solvation structure of Mg ions in dichloro complex solutions from first-principles molecular dynamics and simulated X-ray absorption spectra. *J Am Chem Soc* 2014;136:14456-64. DOI PubMed
  127. Rajput NN, Qu X, Sa N, Burrell AK, Persson KA. The coupling between stability and ion pair formation in magnesium electrolytes from first-principles quantum mechanics and classical molecular dynamics. *J Am Chem Soc* 2015;137:3411-20. DOI PubMed
  128. Canepa P, Gautam GS, Malik R, et al. Understanding the initial stages of reversible Mg deposition and stripping in inorganic nonaqueous electrolytes. *Chem Mater* 2015;27:3317-25. DOI
  129. Xu N, Zhang Y, Zhang T, Liu Y, Qiao J. Efficient quantum dots anchored nanocomposite for highly active ORR/OER electrocatalyst of advanced metal-air batteries. *Nano Energy* 2019;57:176-85. DOI
  130. Qian Z, Li X, Sun B, et al. Unraveling the promotion effects of a soluble cobaltocene catalyst with respect to Li-O<sub>2</sub> battery discharge. *J Phys Chem Lett* 2020;11:7028-34. DOI PubMed
  131. Lai J, Chen N, Zhang F, et al. Imidazolium bromide: a tri-functional additive for rechargeable Li-O<sub>2</sub> batteries. *Energy Stor Mater* 2022;49:401-8. DOI
  132. Hasvold Ø, Henriksen H, Melvåg E, et al. Sea-water battery for subsea control systems. *J Power Sources* 1997;65:253-61. DOI
  133. Yang W, Yang S, Sun G, Xin Q. Development and application of magnesium fuel cell. *CHIN J Power Sources* 2005;29:182-6. Available from: [https://kns.cnki.net/kcms/detail/detail.aspx?dbcode=CJFD&dbname=CJFD2005&filename=DYJS200503016&uniplatform=NZKPT&v=\\_6xHLZPTn7KQ\\_L4mR5bbwgUe\\_uVm87EUswW0qD1\\_FUXTjubNIIHPuVXXJUsbKzBw](https://kns.cnki.net/kcms/detail/detail.aspx?dbcode=CJFD&dbname=CJFD2005&filename=DYJS200503016&uniplatform=NZKPT&v=_6xHLZPTn7KQ_L4mR5bbwgUe_uVm87EUswW0qD1_FUXTjubNIIHPuVXXJUsbKzBw) [Last accessed on 24 Jun 2022].
  134. Cheng C, Li S, Xia Y, et al. Atomic Fe-N<sub>x</sub> coupled open-mesoporous carbon nanofibers for efficient and bioadaptable oxygen electrode in Mg-air batteries. *Adv Mater* 2018;30:e1802669. DOI PubMed